Electronic Supplementary Information

Polythiophene for Near Full pH Photo-antimicrobial

Yunhe Lang,[a] Ying Wang,[a] Ronghui Zhou,[b] Xin Zeng,[b] Hang Zhao,[b] and Peng Wu,*[a,c]

[a]Analytical & Testing Centre, State Key Laboratory of Hydraulics and Mountain River Engineering, Sichuan University, Chengdu 610041, China

[b]State Key Laboratory of Oral Diseases, National Clinical Research Center for Oral Diseases, West China Hospital of Stomatology, Sichuan University, Chengdu 610041, China

[c] School of Chemistry and Chemical Engineering, Henan Normal University, Xinxiang, 453007, China

*Corresponding authors' E-mail: wupeng@scu.edu.cn (P. Wu)

Table of Contents

Section S1. Research Background

Table S1. pH information of various biological tissues and ecological systems

Name	pH range	Ref.
Gastric fluid	1.0 - 3.0	[1]
Vagina	3.8 - 4.5	[2]
Urine	4.5 - 8.0	[3]
Blood plasma	7.35 - 7.45	[1]
Lysosome	4.5 - 5.0	[1]
Freshwater	6.4 - 7.0	[4]
Seawater	~8.1	[5]
Alkaline Lake water	7.2 - 10.1	[6]
Acid lake water	3.6	[7]
Hot spring in Yellowstone	0.5 - 10.5	[8]
Mine wastewater	3.0 - 12.0	[9]
Soil	3.93 - 8.93	[10]

Section S2. Experimental Section

2.1 Materials

Table S2. The information of the purchased materials used in this work.

Name	CAS No.	Specification	Supplier
Methylene Blue	7220-79-3	-	Solarbio, Beijing, China
Ce6	19660-77-6	-	Frontier Scientific
2',4',5',7'-tetraiodofluorescein	16423-68-0	≥90%	Aladdin, Shanghai, China
Dimethyl sulfoxide (DMSO)	67-68-5	≥ 99.95% (GC)	
Riboflavin	83-88-5	≥99%	
Amoxicillin	61336-70-7	USP Grade	Sangon Biotech, Shanghai, China
Cephalexin	15686-71-2	98%	Yuanye Biotech, Shanghai, China
Cefotaxime acid	63527-52-6	98%	
Ciprofloxacin hydrochloride	93107-08-5	88.5%	
Amphotericin B	1397-89-3	USP Grade	
Fluconazole	86386-73-4	99%	
Ketoconazole	65277-42-1	98%	
5-Fluorocytosine	2022-85-7	98%	
Cell Counting Kit-8	-	-	DOJINDO, Japan
Hydrochloric Acid (HCl)	7647-01-0	≥36.5 (AR)	Chron chemicals, Chengdu, China
Sodium hydroxide (NaOH)	1310-73-2	AR	
Acetonitrile (CH_3CN)	75-05-8	GC	
Phosphate Buffer Saline	-	1x	KeyGEN Bio TECH, Nanjing, China

2.2 Instrumental Information

Table S3. The instrumental information used for characterizations in this work.

Characterization items	Type	Manufacturer
UV/Vis absorption spectra	Lambda-365	Perkin Elmer, USA
Fluorescence	FluoroMax-4P spectrofluorometer	Horiba Scientific, USA
Fluorescence lifetime	Fluolog-3 spectrofluorometer Fluorescence lifetime excitation: DeltaDiode 405L	Horiba Jobin Yvon, USA
$^1O_2$ phosphorescence emission	Fluolog-3 spectrofluorometer NIR Detector excitation: 445 nm laser	Horiba Jobin Yvon, USA
Transient absorption spectra	EOS fire	Ultrafast Systems, USA
Microplate Reader	Multiskan FC	Thermo, Shanghai
Cell Imaging	Nikon A1+	Nikon, Japan
HE Staining	Eclipse Ci-L	Nikon, Japan
Zeta Potential	Zetasizer Nano ZS	Malvern, England
SEM	Aztec Live ULTIM	Oxford Instruments, England
pH meter	FE20	METTLER TOLEDO, Shanghai
Lasers	445 nm, MXL-III-445	Changchun New Industries Optoelectronics Technology Co., Ltd.
	532 nm, MGL-FN-532	
	660 nm, MRL-III-660D	

2.3 Methods

Synthesis of PT10. The PT10 photosensitizer was synthesized and purified according to the previous publication.[11]

pH titration. Photosensitizers and antibiotics were dissolved to obtain 1 mM stock solutions, and then diluted to work concentrations (abs = 0.2-0.8). The media pH of the above solutions (0-14) was adjusted with HCl (1.0 M) or NaOH (1.0 M). After collection of the pH-dependent absorption and fluorescence spectra, K_a was calculated used by the sigmoidal fitting model[12]. For $^1O_2$ phosphorescence emission, pH of the solutions was adjusted with concentrated HCl or NaOH solution dissolved in D_2O (1.0 M). The 445 nm laser (PT10, riboflavin, and Ce6), 532 nm laser (TIF) and 660 nm laser (MB) were employed for excitation, and the $^1O_2$ phosphorescence emission (1275 nm) were then collected.

Stability evaluation. Long-term stability of the antimicrobials (7 days) was evaluated through the absorption change at pH 2, 4, 7, and 12. Photostability of the photosensitizers (pH = 2, 7, and 12) were measured using a 445 nm laser (PT10, riboflavin, and Ce6), a 532 nm laser (TIF) and 660 nm laser (MB) as the light source (30 mW/cm^2). Before measurements, the absorbance of the photosensitizers was set the same at the excitation wavelengths to ensure the same the same exciton density.

Microbials culture. The detailed information about the Microbial strains used in this work were listed in Table S4 below. All microbials were cultured anaerobically in liquid

culture medium (170 r/min) except *H. pylori* and *M. aeruginosa*. *H. pylori* was cultured on a Columbia agar plate containing 6.5% sheep blood, 0.84% brain heart immersion, and multiple antibiotics under growth at 37 ℃ (5% O_2, 10% CO_2, 85% N_2) for 3-5 days. *M. aeruginosa* was purchased from the Institute of Hydrobiology, Chinese Academy of Sciences (strain number, FACHB-526). Cells were cultured in flasks using BG11 culture medium at 25 ℃ with a 12 h light/12 h dark (2000 Lux).

Table S4. Information about the microbials in this work.

Characterization items	Microbials name	pH	Culture medium	Incubation time / h	Culture Temperature / ℃
Gram positive (G+)	*Staphylococcus aureu*	7.0	LB	12	37
	Methicillin-resistant Staphylococcus aureu	7.0	LB	12	37
	Alicyclobacillus acidoterrestris	4.0	BAT	24	45
Gram negative (G-)	*Helicobacter pylori*	2.0	Columbia, Brain heart immersion, sheep blood and multiple antibiotics	72-120	37
	Escherichia coli	7.0	LB	12	37
	Penicillin-resistant Escherichia coli	7.0	LB	12	37
Fungus	*Candida albicans*	2.5	PDA	30	37
Cyanobacteria	*Microcystis aeruginosa*	12	BG-11	-	25

Antimicrobial experiments *in vitro*. The bacterial or fungus suspension was diluted into a desired concentration according to the optical density at 600 nm. Then, photosensitizers of varied concentrations were added into the above suspensions,

followed by light illumination with LED (30 mW/cm^2, 10 min). Finally, for colony-forming units (cfu) counting, the treated microbials liquid (100 μL) was smeared onto agar plates for culturing.

The photo-inactivation of *M. aeruginosa* with PT10 and other photosensitizers were carried out in NaOH solution (pH = 12). The initial concentration of the algal suspension was determined by the Neubauer haemocytometer through cell counting (9 × 10^6 cell/mL, $OD_{680\ nm} \approx 0.23$). The photosensitizers were set at the same absorbance (abs = 0.3) at the wavelength maxima. During illumination, the cell samples was placed in a constant temperature oscillator (25 ℃, 200 r/min). Samples were taken at different time intervals (0-1 h), and the inhibition efficiency was evaluated through the decreased absorption at 680 nm.

Determination of MICs and IC_{50}s. In brief, the microbial liquid (100 μL, 10^5 cfu/mL) were added into the culture medium, followed by the addition of 20 μL of the culture medium containing serial concentrations of a given antimicrobial. Afterwards, the microbials were subjected to LED irradiation for 10 min, and then cultured in a 24-well plate. The media pH was adjusted with HCl (1 M) to evaluate the effect of pH to MICs (pH 5.0-7.0). Microbials without any treatment were set as the control. After incubation, the OD_{600} of the antimicrobials was measured for calculation of MIC and IC50 of the photosensitizers. For antibiotics, the processes were generally the same as above, except LED irradiation.

Preparation of microbial samples for SEM. *C. albicans* or *M. aeruginosa* (~10^6 cfu/mL) was exposed to a lethal dose of PT10 and blue light as above, with treatment with blue light alone as the controls. The microbials were collected by centrifugation and washed with PBS for three times after treatments. Then, the cells were fixed with 2.5% glutaraldehyde for 2-3 h at room temperature, followed by sequential dehydration with increasing concentrations of ethanol (20%, 30%, 50%, 75%, 90% and 100% for 10 min, respectively). The obtained solution was dropped onto the conductive silicon and examined with SEM after dried.

Cytotoxicity assay. A549 cells and L929 cells were cultured in DMEM supplemented with 10% FBS at 37 ℃ in a humid atmosphere containing 5% CO_2, followed by seeding in 96-well plates (10^4 cells/mL) for adherent growth (24 h). Afterwards, the cells were washed with PBS, and a series of concentrations of PT10 (100 μL) were then added. After incubation for 24 h, the supernatant was removed, and the adherent cells were further washed with PBS. To evaluate the cell vitality, CCK-8 (DOJINDO, Japan) was added and incubated for 0.5 h at 37 ℃. The absorbance at 450 nm was recorded with a microplate reader (Thermo, Shanghai).

***In vivo* photo-antimicrobial evaluation of PT10.** Healthy female ICR mice (20-25 g) were used under approved by the Subcommittee on Research and Animal Care of Sichuan University (code: WCHSIRB-D-2021-346). The loading of *C. albicans* was based on the method described previously with minor modifications.[13] The animals were divided into six groups (n = 6 per group: normal, dark, PT10, light, PT10 + light,

and riboflavin + light). Mice were susceptible to oropharyngeal candidiasis infection after intramuscular injection of cortisone acetate (125 mg/kg, day -1 and day 1 relative to infection). To prevent unknown bacterial infections, 0.83 g/L tetracycline hydrochloride was added to drinking water for mice. To construct the infection model, the mice were inoculated by cotton balls with *C. albicans* (10^6 cfu/mL) for 90 min at day 0. PT10 (50 μL, 20 μg/mL) in pH 2.0 media were smeared onto the oral mucosa and treated with 445 nm light (50 mW/cm^2, 12 min) at day 1 and day 2. To evaluate the photo-antimicrobial therapy effect, the body weight, pathology index, and colonies of *C. albicans* were evaluated every day. At day 5, one mouse per group was sacrificed for H&E staining and PAS staining analysis in the infected tongue.

Section S3. pH responsiveness of antimicrobials

3.1 PT10

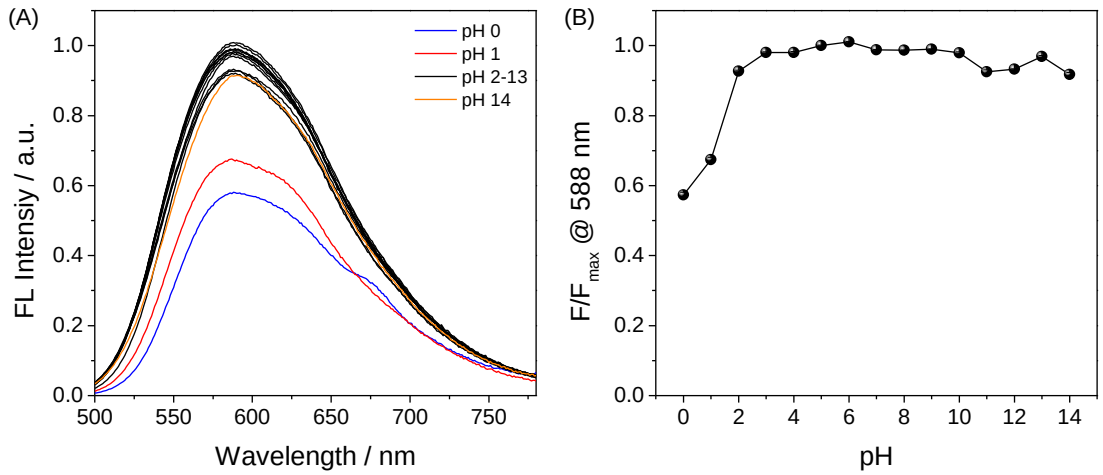

Figure S1. (A) fluorescence emission spectra (λ_{ex} = 400 nm) and (B) the fluorescence emission intensity (λ_{em} = 588 nm) of PT10 in the pH range of 0-14.

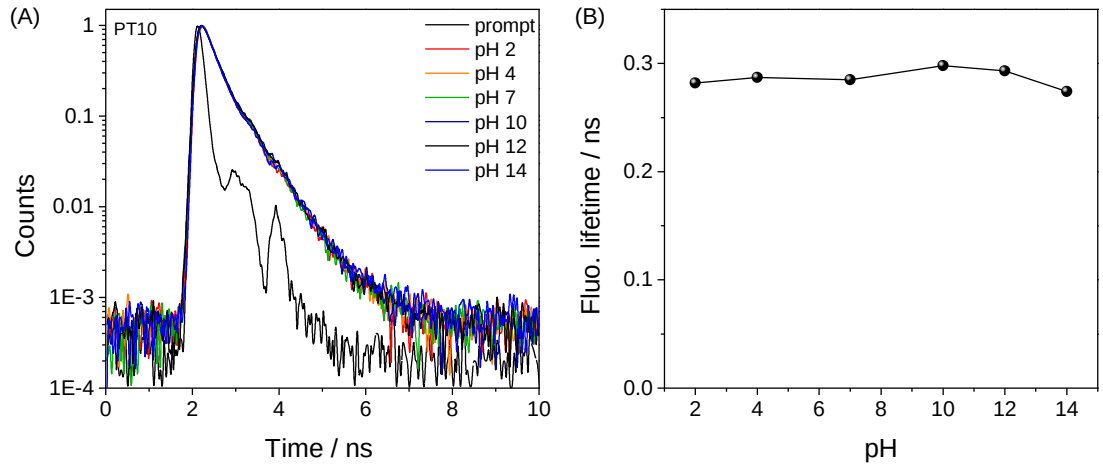

Figure S2. (A) Fluorescence decay of PT10; (B) fluorescence lifetime of PT10 at different pH (from acid to alkaline).

3.2 Antibiotics

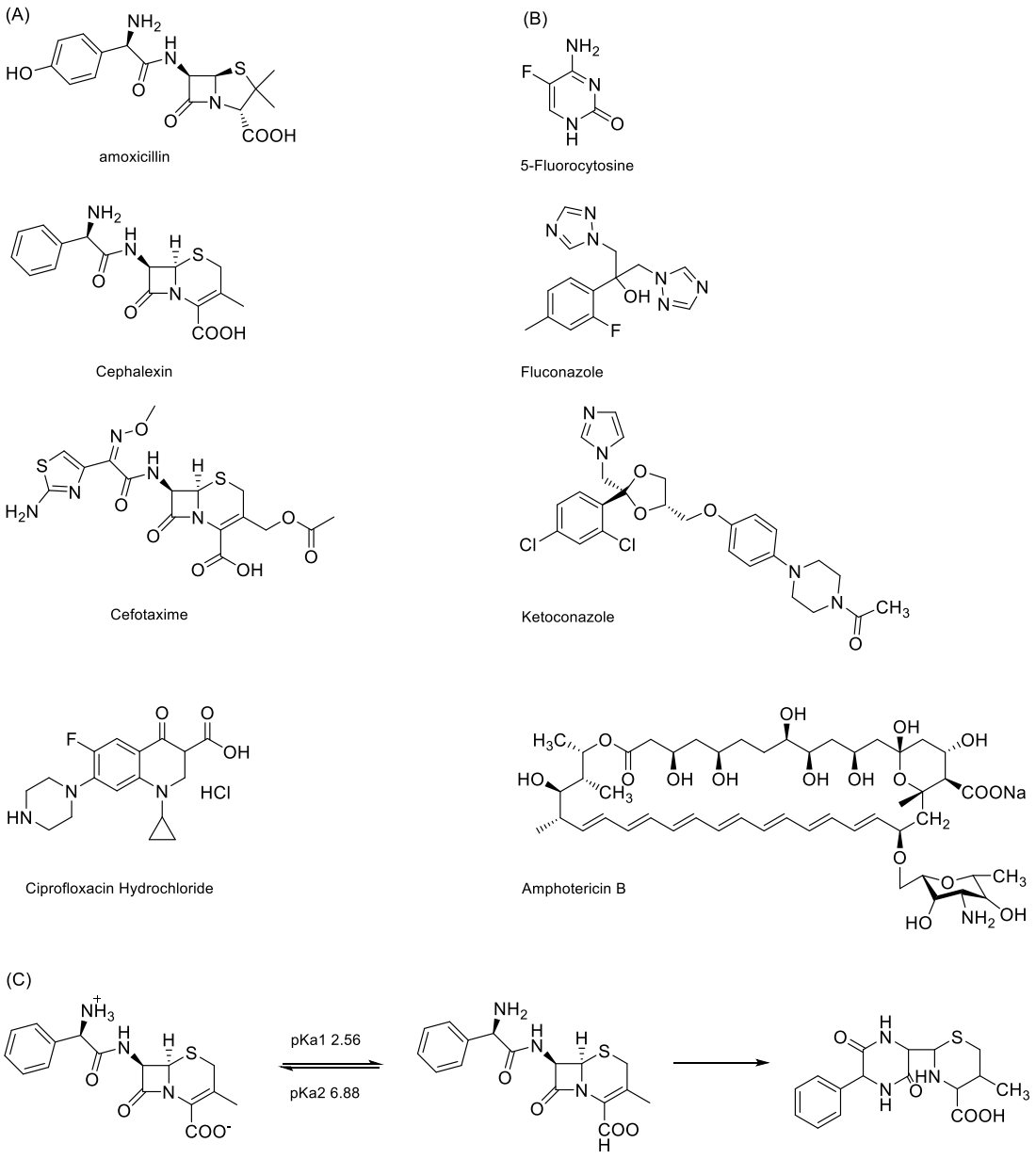

Figure S3. (A) The structures of several broad-spectrum bacterial antibiotics, (B) broad-spectrum fungus antibiotics; and (C) structural change of Cephalexin in extremely acidic condition.

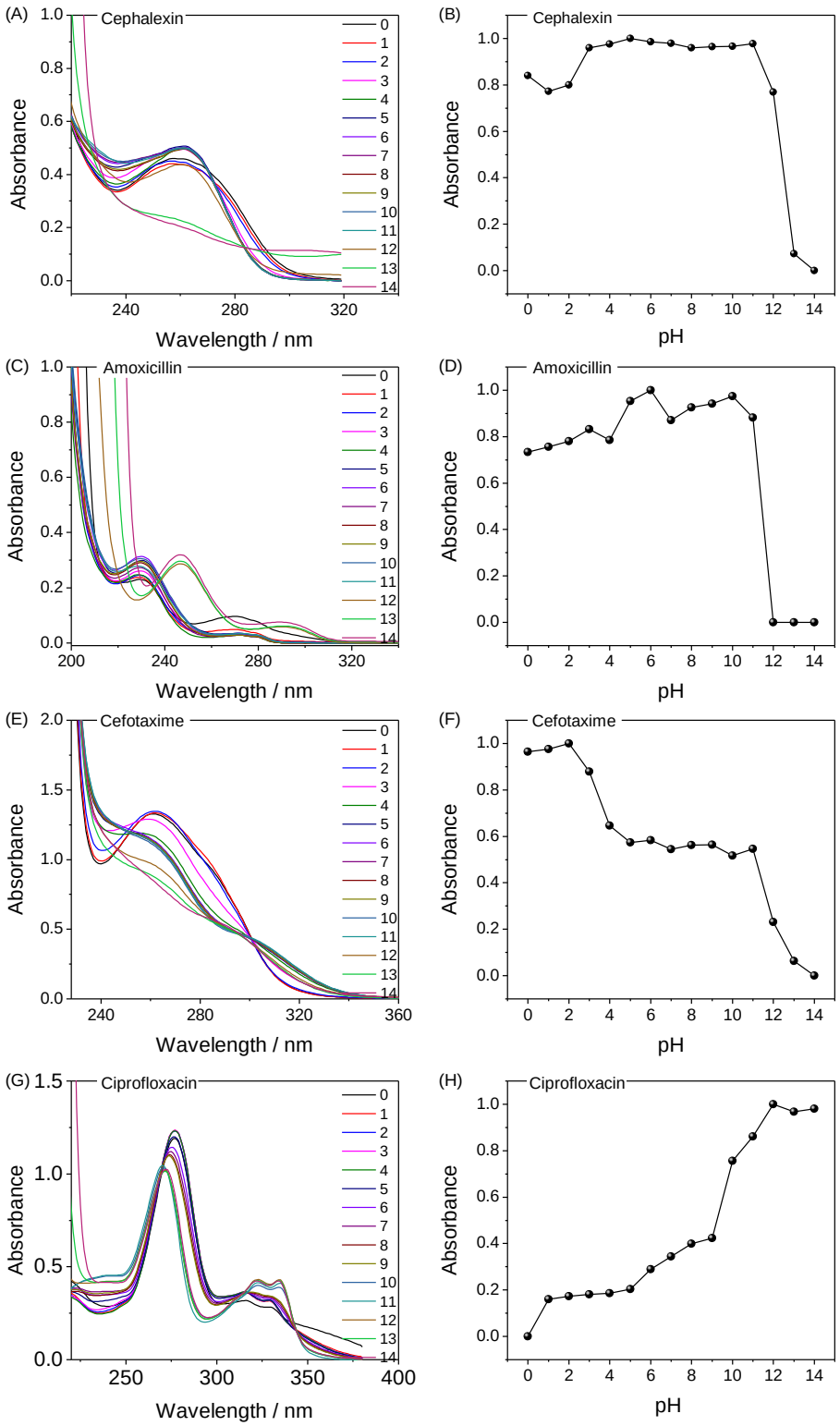

Figure S4. The pH-dependent absorption spectra and absorbance at the maximum absorption wavelength of bacteria antibiotics: (A-B) Cephalexin, (C-D) Amoxicillin, (E-F) Cefotaxime and (G-H) Ciprofloxacin.

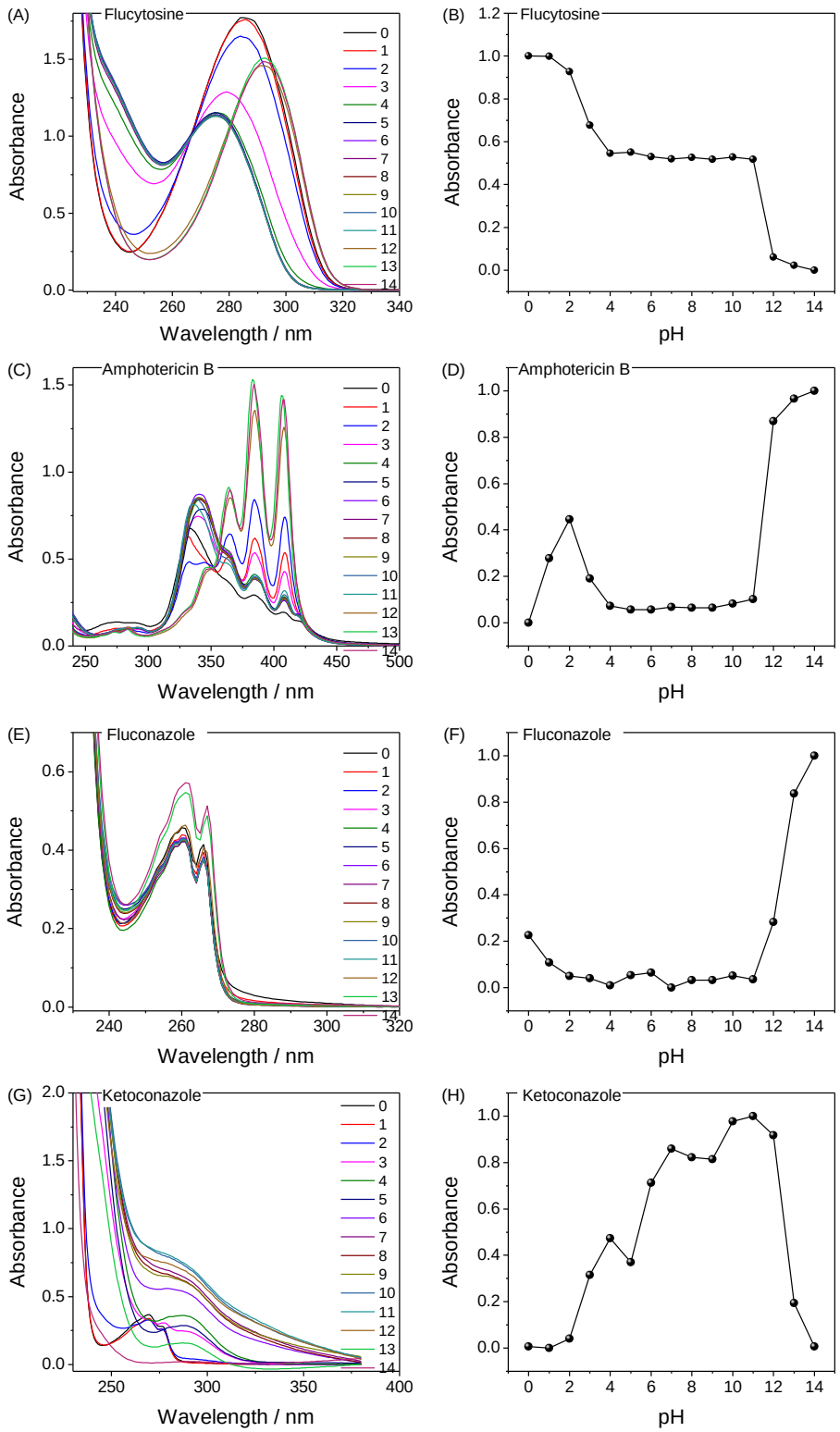

Figure S5. The pH-dependent absorption spectra and absorbance at the maximum absorption wavelength of fungus antibiotics: (A-B) Flucytosine, (C-D) Amphotericin B, (E-F) Fluconazole and (G-H) Ketoconazole.

3.3 Common photosensitizers

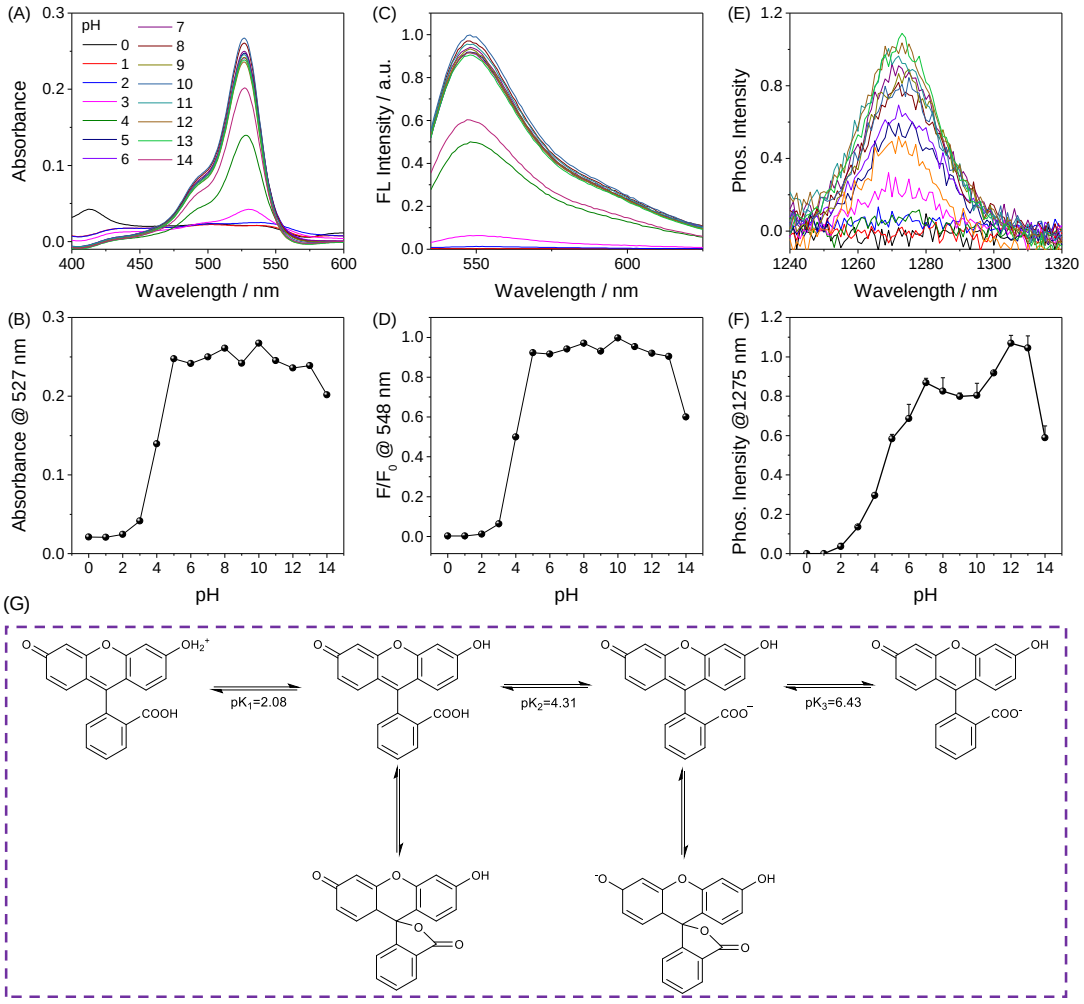

Figure S6. The pH-dependent photophysical properties of TIF: (A-B) absorption spectra; (C-D) fluorescence spectra; (E-F) the 1275 nm phosphorescence emission of $^1O_2$; and (G) the pH-dependent chemical structure change of xanthenes. The open-ring structure is the most stable colored and fluorescent form, whereas intramolecular spirocyclization with protonation process is color less and non-fluorescent.[14]

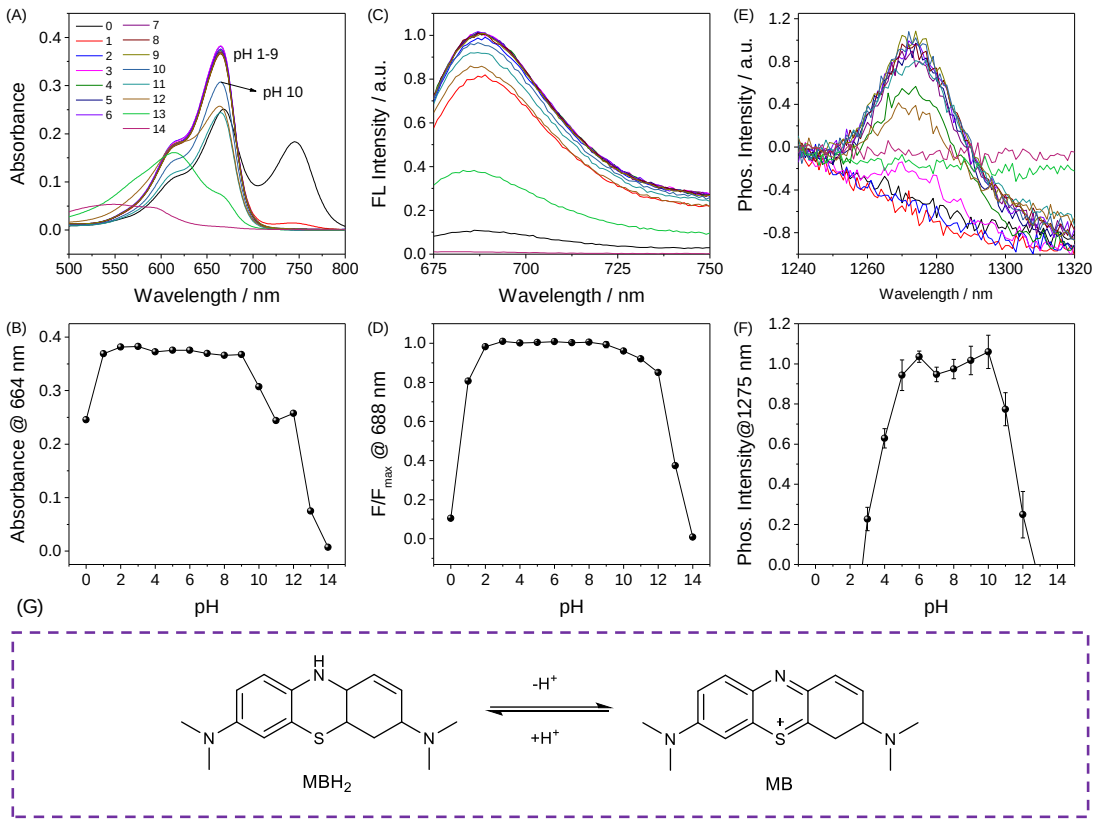

Figure S7. The pH-dependent photophysical properties of MB: (A-B) absorption spectra; (C-D) fluorescence spectra; (E-F) the 1275 nm phosphorescence emission of $^1O_2$; and (G) the pH-dependent chemical structure change of MB. MB was reduced under acidic conditions and the reduced species, MBH_2, is non fluorescence under visible excitation.[15]

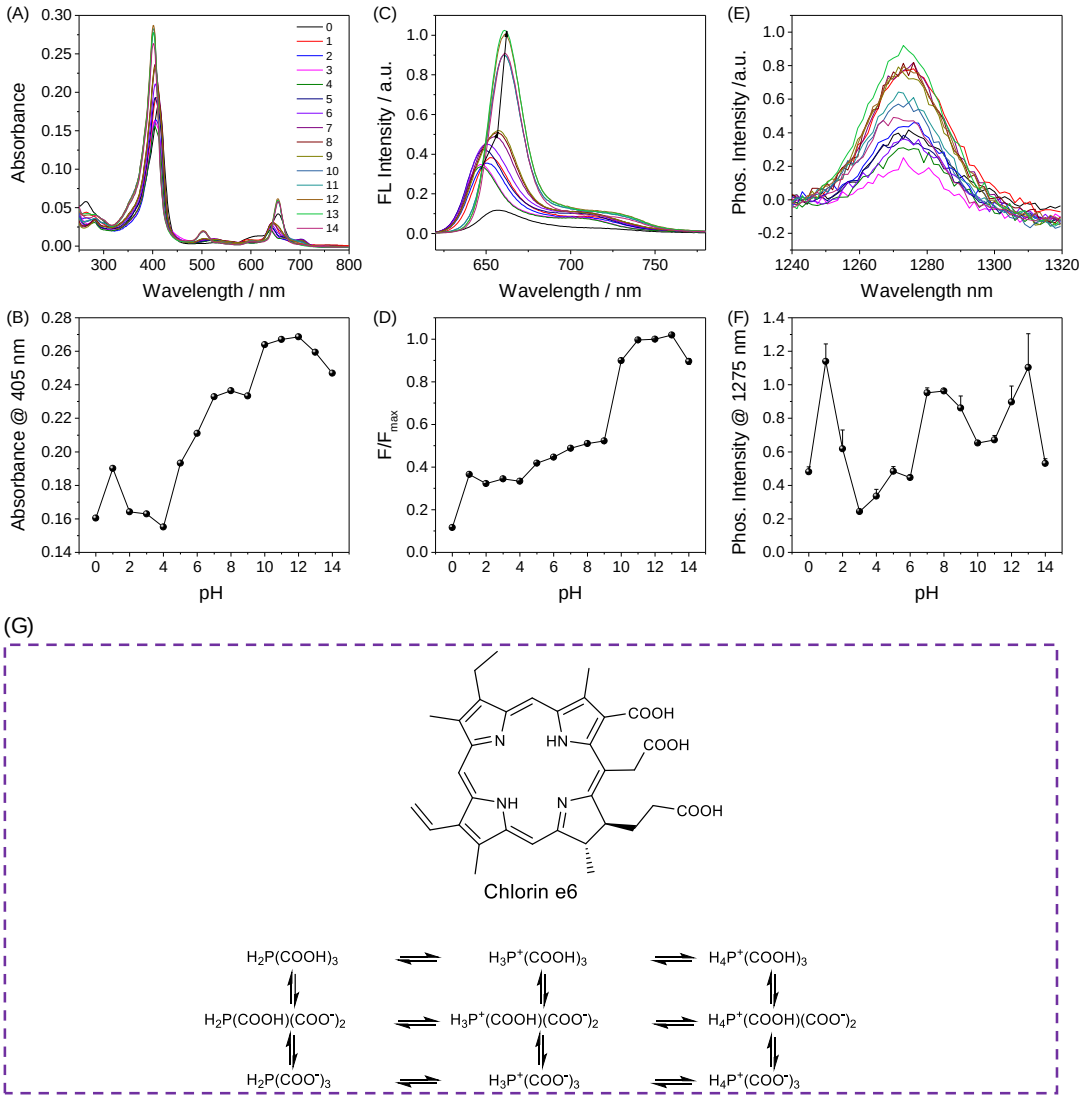

Figure S8. The pH-dependent photophysical properties of Ce6: (A-B) absorption spectra; (C-D) fluorescence spectra; (E-F) the 1275 nm phosphorescence emission of $^1O_2$; and (G) the pH-dependent chemical structure change of Ce6 (protonation and self-aggregation process in acidic and neutral conditions[16a, 16b]).

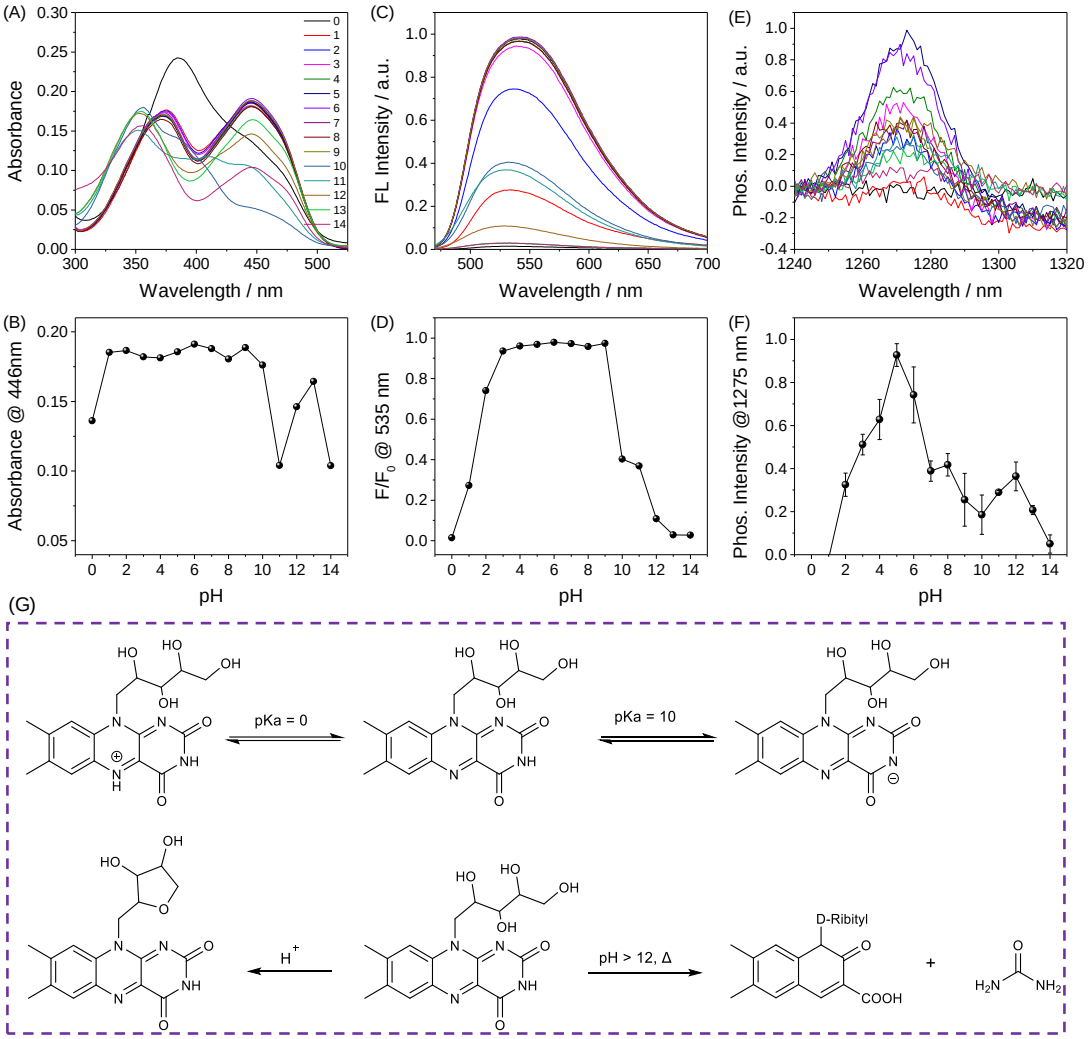

Figure S9. The pH-dependent photophysical properties of riboflavin: (A-B) absorption spectra; (C-D) fluorescence spectra; (E-F) the 1275 nm phosphorescence emission of $^1O_2$; and (G) the pH-dependent chemical structure change of riboflavin (protonation/deprotonation process and even degradation process[17]).

3.4 MEP and PA of PT10 monomer and PT10-no NH_4^+

Molecular electrostatic potential (MEP) for ground state PT10 monomer and PT10 monomer without quaternary ammonium (PT10-no NH_4^+) were used to evaluate the protonation reactivity. Geometry optimization was calculated using density functional theory (DFT) with B3LYP functional and 6-31G** basis set with Gaussian 09. Solvent phase calculations were carried out using Polarized Continuum Model (PCM). Quantitative analysis of molecular surface was calculated at Multiwfn software package[18a, 18b]. Visualization of MEP map were performed with VMD software package.

For the gas-phase proton affinity (PA), the gas geometry optimization was carried out using DFT with B3LYP/6-31G*. And the energy was carried out using DFT with M06-2X/def2TZVP. The gas-phase proton affinity (PA) has been calculated for the following reaction:[19]

$$B + H^+ \leftrightarrow BH^+$$

where B is the base form and BH^+ is the protonated form. The PAs were calculated using:

$$PA = -\Delta H = \Delta E + \Delta ZPE + \frac{5}{2}RT$$

where ΔH is the enthalpy change of the protonation reaction, E is the electron energy at 0 K, ZPE is the zero point correction, R is the molar gas constant, and T is the absolute temperature in kelvin.

Table S5. Calculated proton affinities of PT10 and PT10-NH_4^+ oligomers

	Energy/ hartree	ZPE / hartree	PA / hartree	PA / kJ/mol
PT10-no NH_4^+ Monomer	-1177.1083	0.4571	0.3329	874
PT10-no NH_4^+ Monomer (H^+)	-1177.4516	0.4698		
PT10 Monomer	-1350.7488	0.5797	0.2414	634
PT10 Monomer (H^+)	-1351.0001	0.5920		
PT10-no NH_4^+ Dimer	-2353.0335	0.8939	0.3579	940
PT10-no NH_4^+ Dimer (H^+)	-2353.4019	0.9086		
PT10 Dimer	-2700.2834	1.1392	0.2186	574
PT10 Dimer (H^+)	-2700.5120	1.1515		

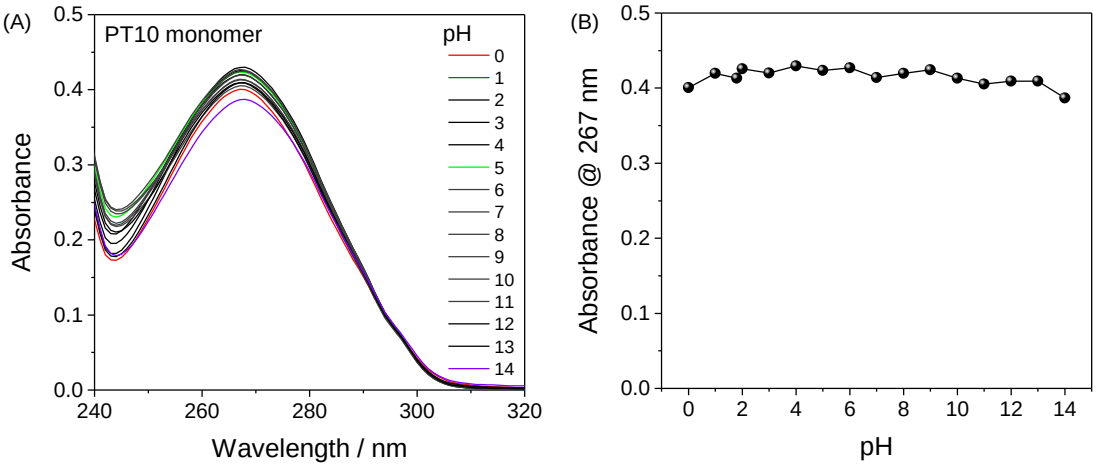

Figure S10. (A) UV-vis absorption spectra and (B) the absorbance (267 nm) of PT10 monomer in the pH range of 0-14.

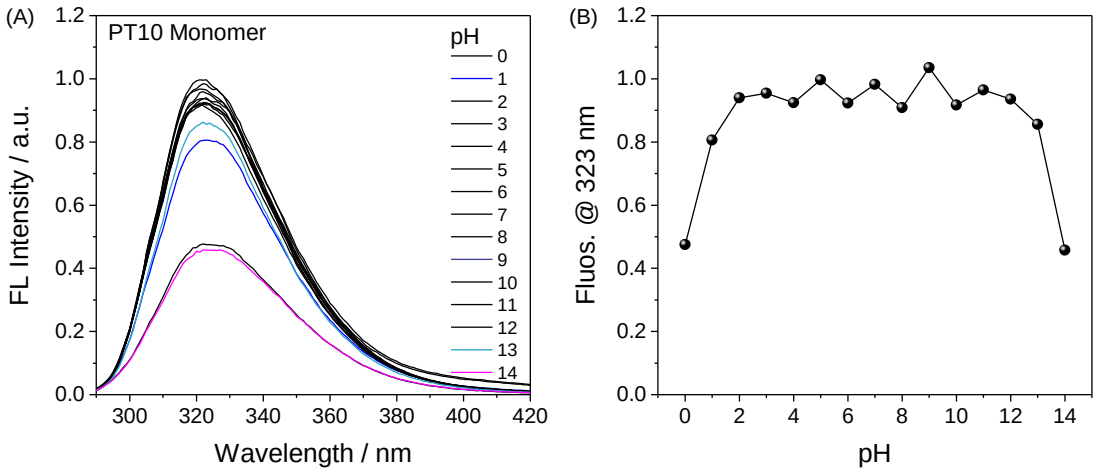

Figure S11. (A) fluorescence emission spectra (λ_{ex} = 270 nm) and (B) the fluorescence emission intensity (λ_{em} = 328 nm) of PT10 in the pH range of 0-14.

3.5 Other polythiophenes

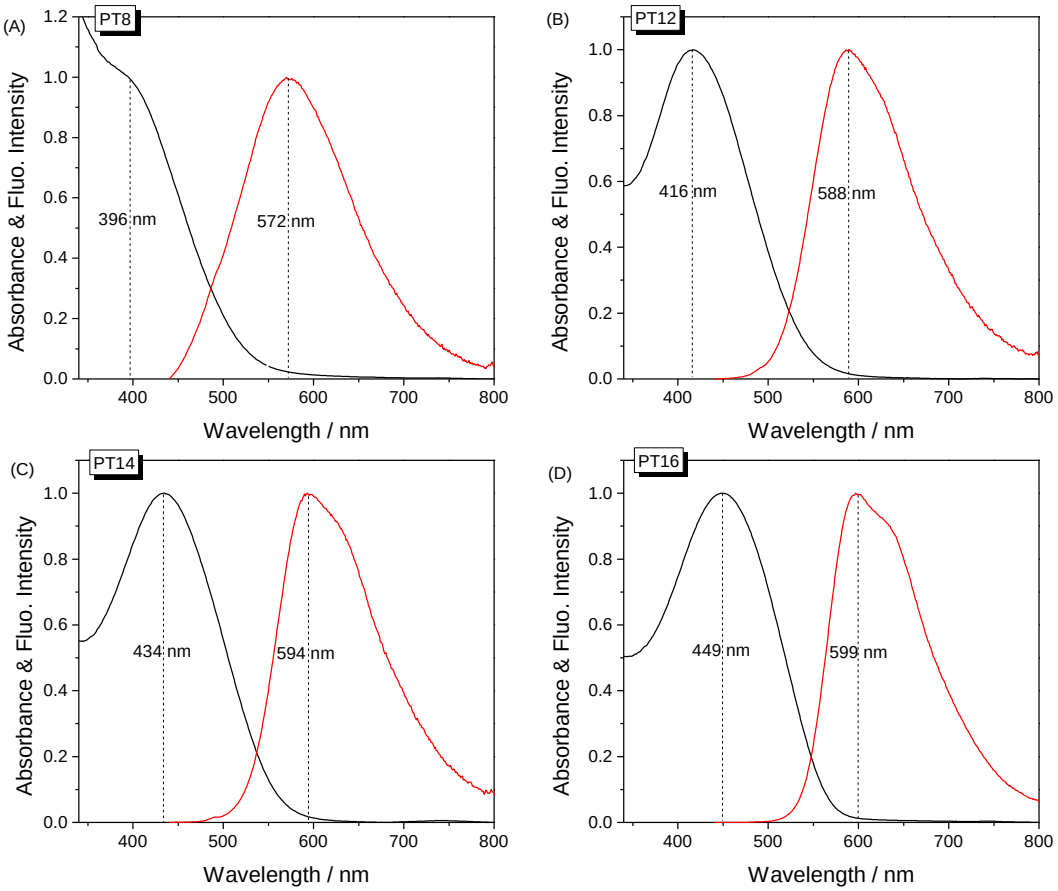

Figure S12. The absorption and fluorescence spectra of (A) PT8, (B) PT12, (C) PT14, and (D) PT16

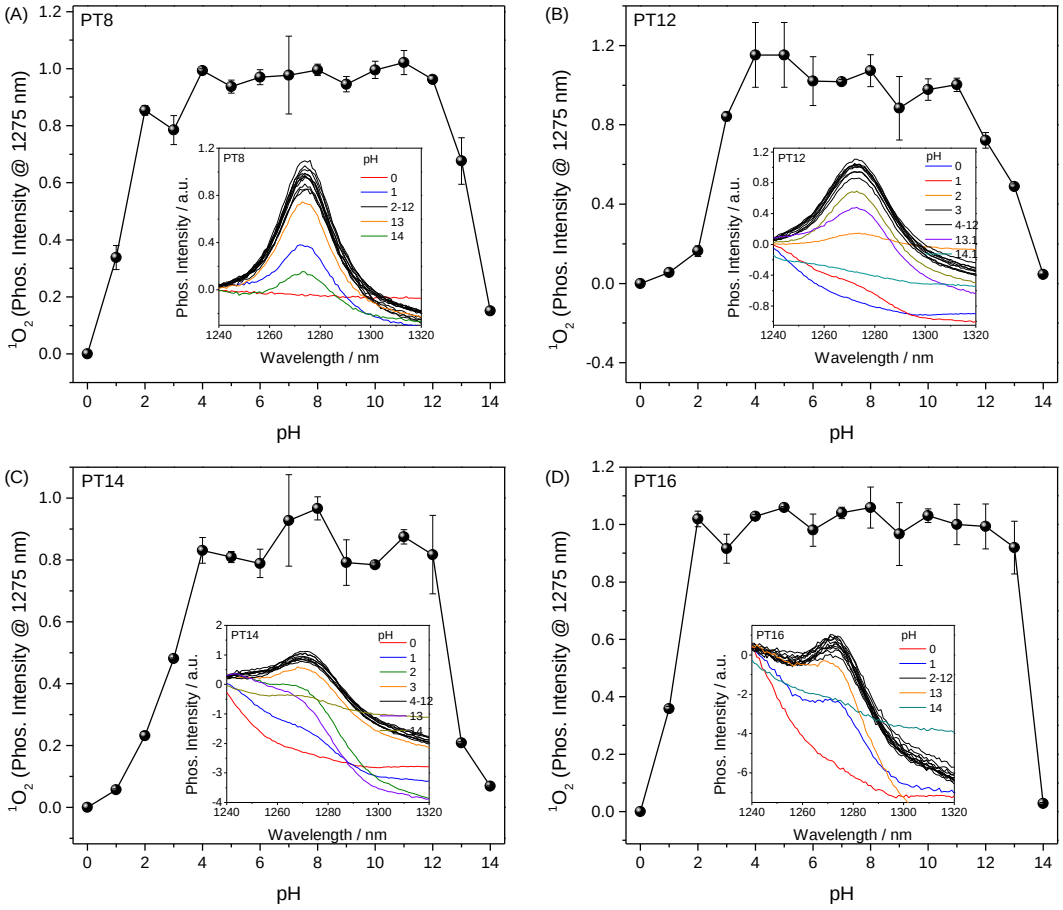

Figure S13. pH-dependent $^1O_2$ generation (revealed by the characteristic 1275 nm phosphorescence emission) of (A) PT8, (B) PT12, (C) PT14 and (D) PT16 (inset: the corresponding phosphorescence emission of $^1O_2$ in D_2O, excited with a 445 nm laser).

Section S4. pH-dependent long-term stability and photostability

4.1 Long-term stability of photosensitizers

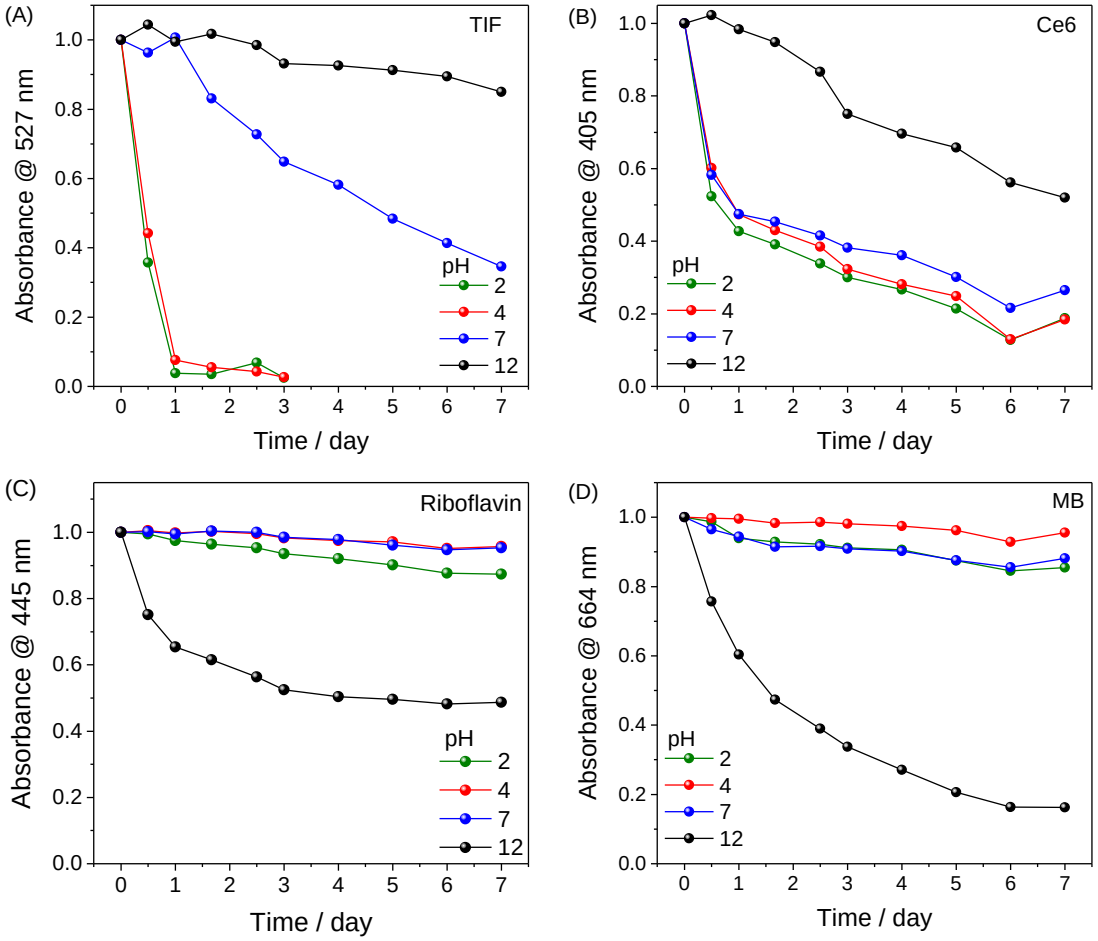

Figure S14. Time-courses (7 days) of the absorbance change of TIF (A), Ce6 (B), riboflavin (C), and MB (D) at pH 2, 4, 7 and 12.

4.2 Long-term stability of antibiotics

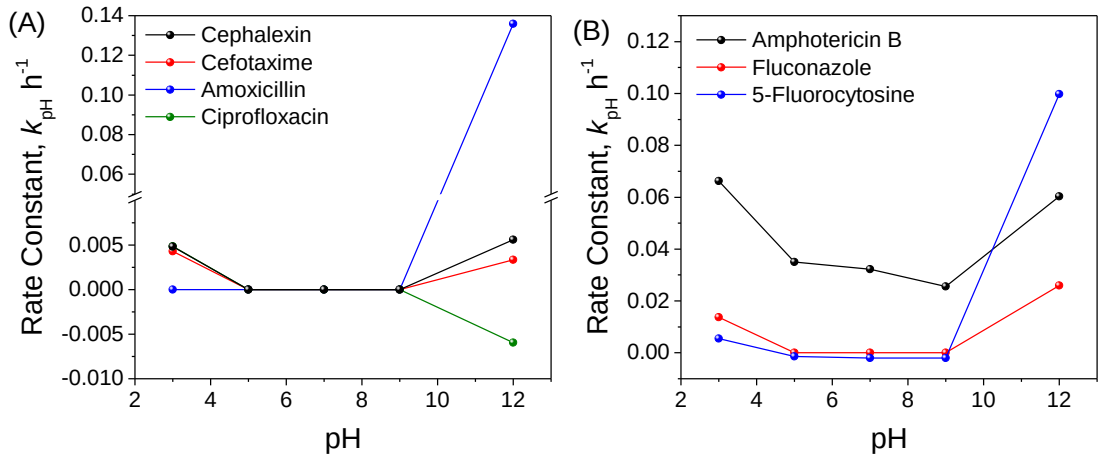

Figure S15. The hydrolysis rates of antibiotics (determined by UV-Vis absorption spectra): (A) bacterial antibiotics and (B) fungi antibiotics at different pH.

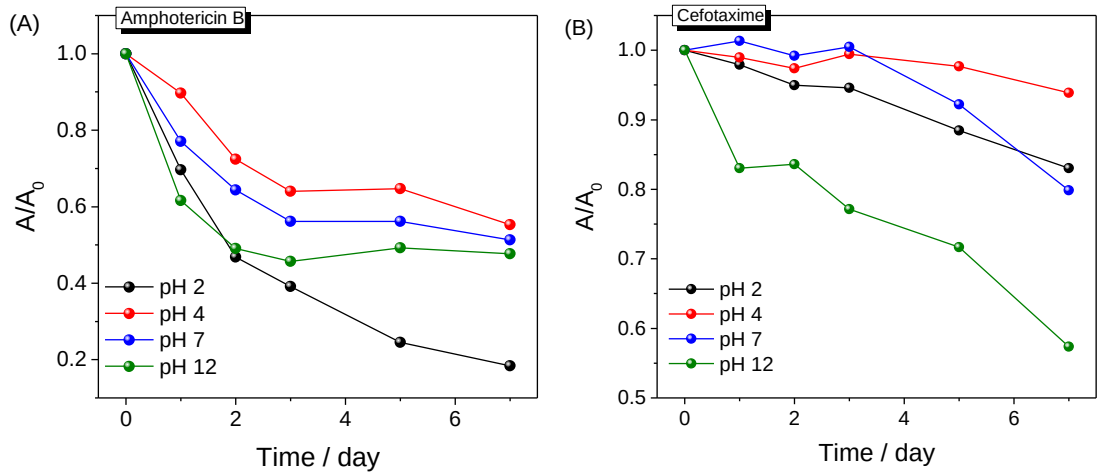

Figure S16. Time-courses (7 days) of the absorbance change of Amphotericin B (A) and Cefotaxime (B) at pH 2, 4, 7 and 12.

4.3 Photo-stability of photosensitizers

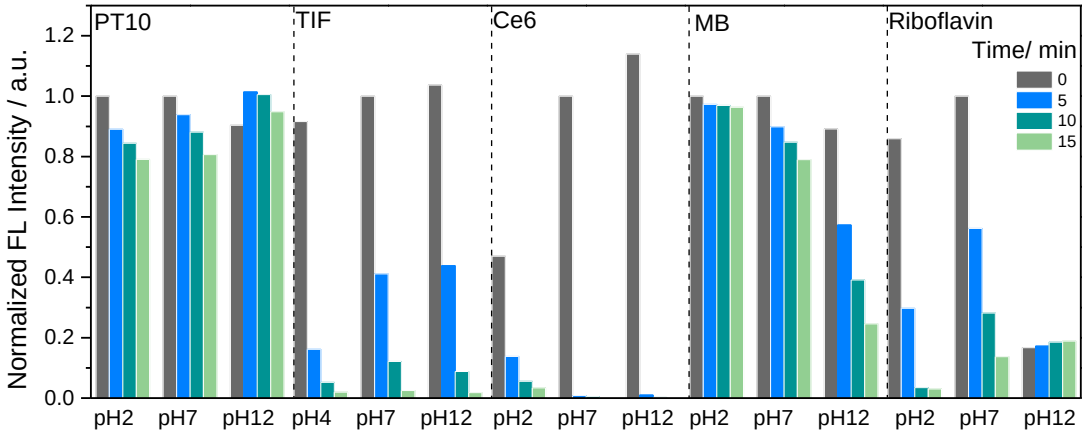

Figure S17. Evaluation of the photo-stability of PT10 and other photosensitizers at different pH via their corresponding fluorescence intensity.

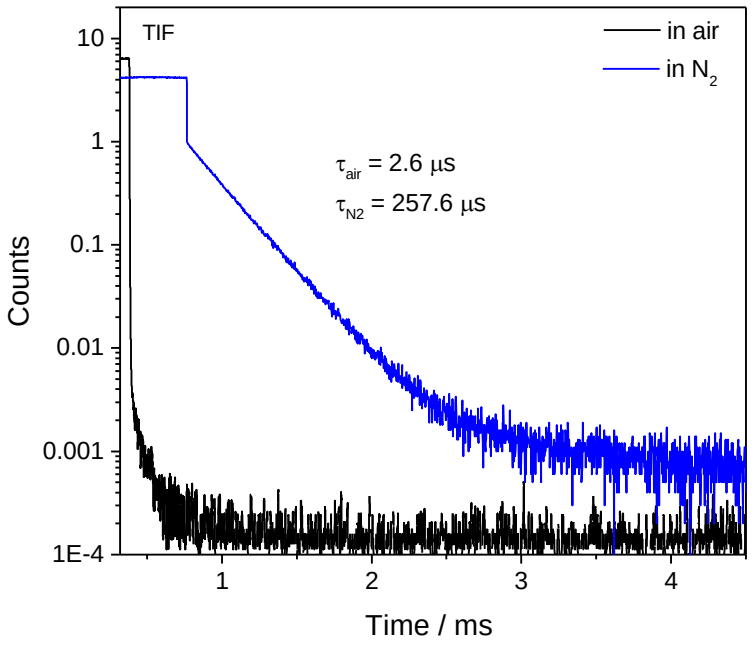

Figure S18. Phosphorescence decays of TIF in air and N_2-saturated solution.

Table S6. Excited triplet state lifetime ($\tau_{In\ N2}$/ $\tau_{In\ air}$) of PT10 and photosensitizers

Photo-antimicrobials	$\tau_{In\ air}$ / μs	$\tau_{In\ N2}$ / μs	$\tau_{In\ N2}$ / $\tau_{In\ air}$	References
PT10	1.4	10.5	7.5	[20]
TIF	2.6	257.6	99.1	Figure S18
Ce6	3.0	180.0	60.0	[21]
MB	1.8	79.5	44.2	[22]
Riboflavin	3	-	-	[23]

Section S5. Photo-antimicrobial performance of PT10

5.1 PT10

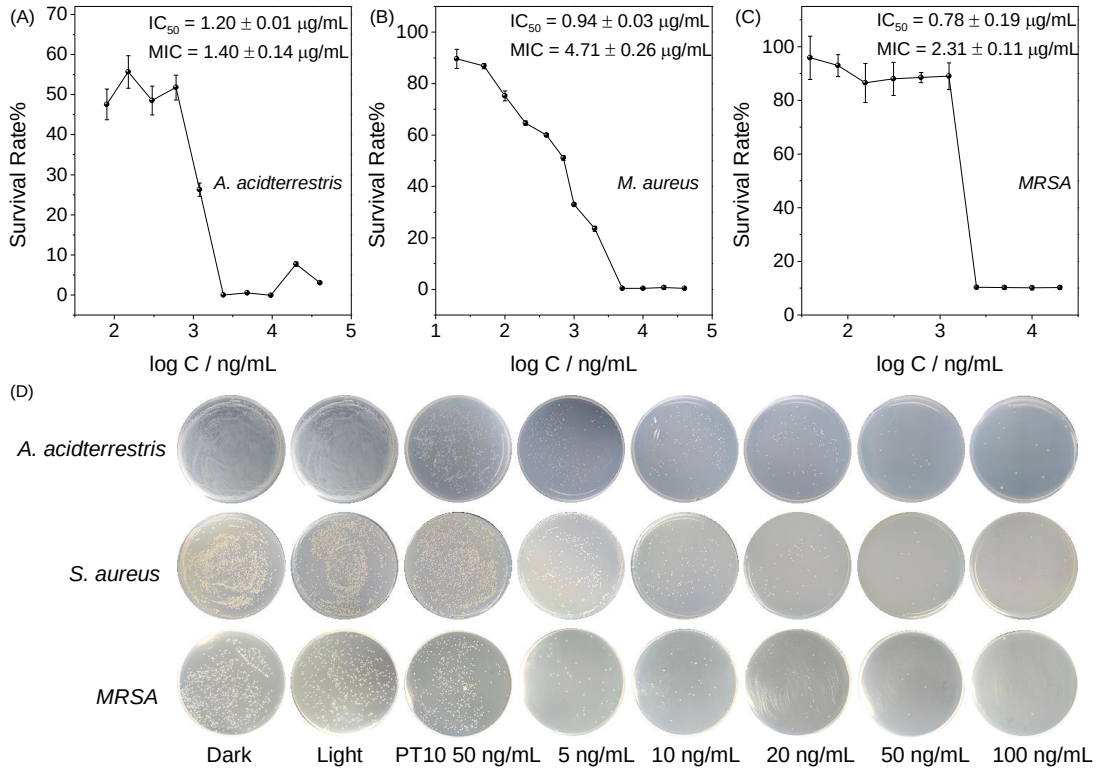

Figure S19. PDI performance of PT10 (concentration-dependent) for G positive bacteria: (A) *A. acidterrestris*; (B) *S. aureus*; (C) *MRSA*; and (D) photographs of *A. acidterrestris*, *S. aureus*, and *MRSA* colonies, respectively. Irradiation: 450 nm (LED, 30 mW/cm^2) for 10 min. Error bar = Standard Deviation (n = 3).

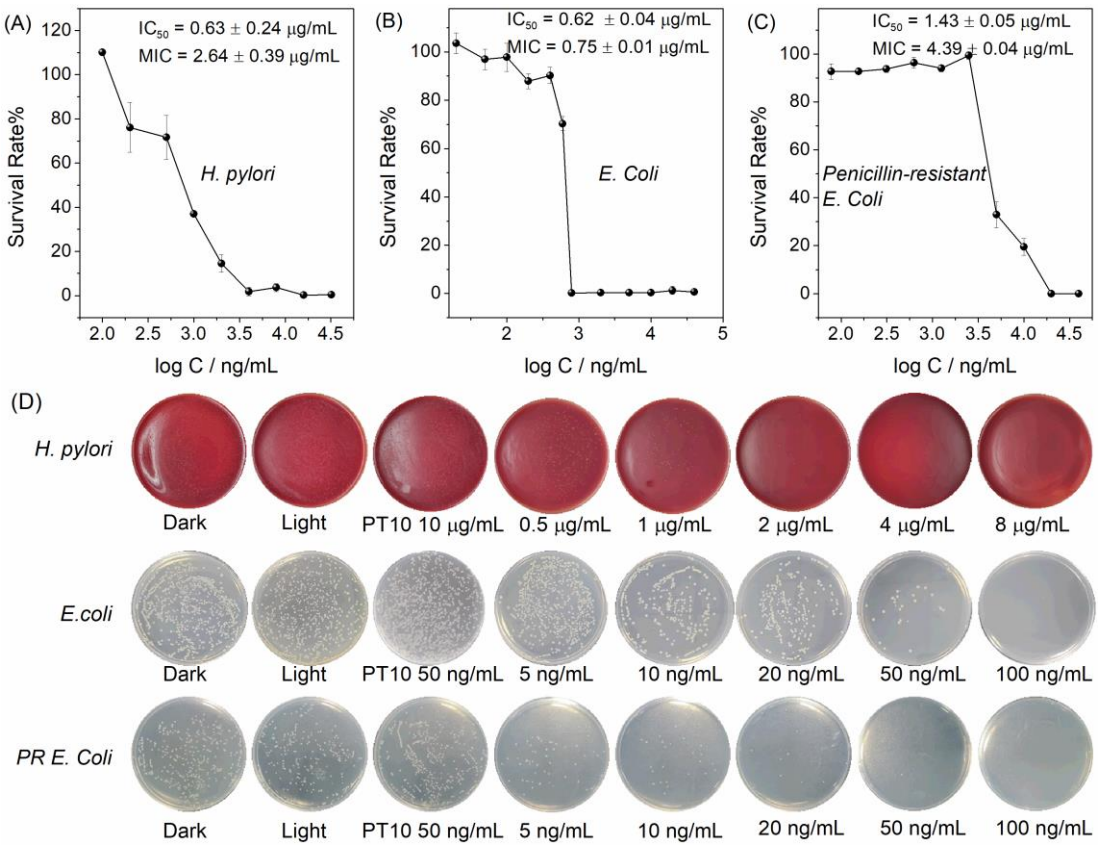

Figure S20. PDI performance of PT10 (concentration-dependent) for G negative bacteria: (A) *H. pylori*; (B) *E. coli*; (C) *Penicillin-resistant E. coli*; and (D) photographs of *H. pylori*, *E. coli*, and *Penicillin-resistant E. coli* colonies, respectively. Irradiation: 450 nm (LED, 30 mW/cm^2) for 10 min. Error bar = Standard Deviation (n = 3).

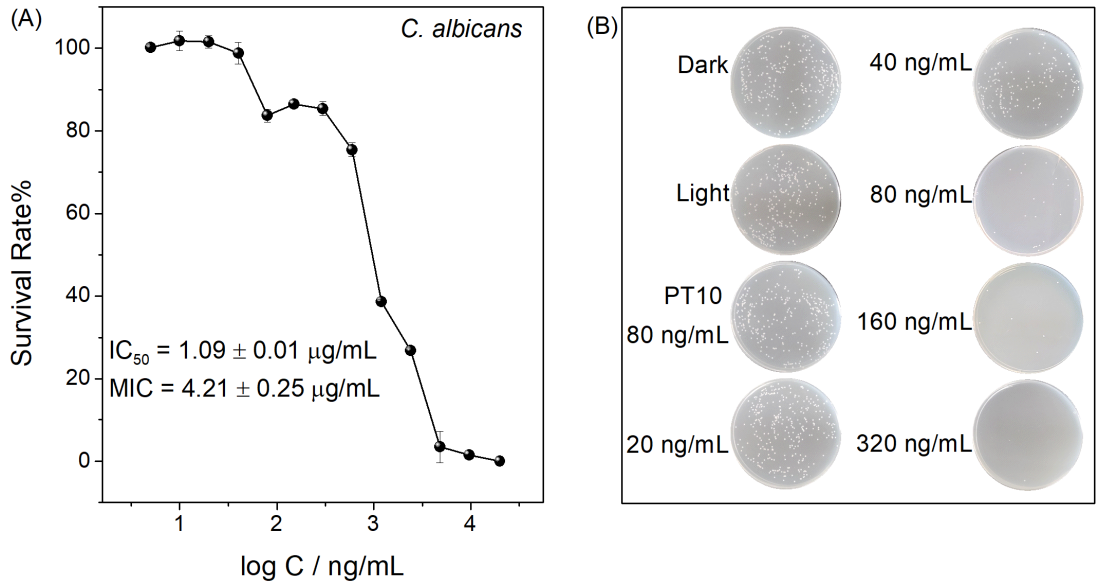

Figure S21. PDI performance of PT10 for fungal (*C. albicans*): (A) concentration-dependent-inactivation of *C. albicans*; and (B) photographs of *C. albicans* colonies. Irradiation: 450 nm (LED, 30 mW/cm^2) for 10 min. Error bars = Standard Deviation (n = 3).

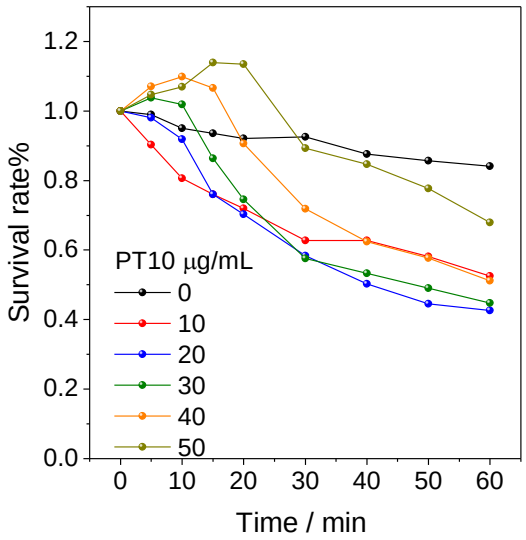

Figure S22. PDI performance of PT10 for cyanobacterial *M. aeruginosa*: time courses of the survival rates of *M. aeruginosa* with different concentrations of PT10.

Table S7. The essential information of microbials in this work.

Characterization items	Microbials name	MIC_{100} μg/mL	IC_{50} μg/mL
Gram positive (G+)	*Staphylococcus aureu*	4.71 ±0.26	0.94 ±0.03
	Methicillin-resistant Staphylococcus aureu	2.31 ±0.11	0.78 ±0.19
	Alicyclobacillus acidoterrestris	1.40 ±0.14	1.20 ±0.01
Gram negative (G-)	*Helicobacter pylori*	2.64 ±0.39	0.65 ±0.24
	Escherichia coli	0.75 ±0.01	0.62 ±0.04
	Penicillin-resistant Escherichia coli	4.39 ±0.04	1.43 ±0.05
Fungus	*Candida albicans*	4.21 ±0.25	1.09 ±0.01
Cyanobacteria	*Microcystis aeruginosa*	-	30 μg/mL 30 min

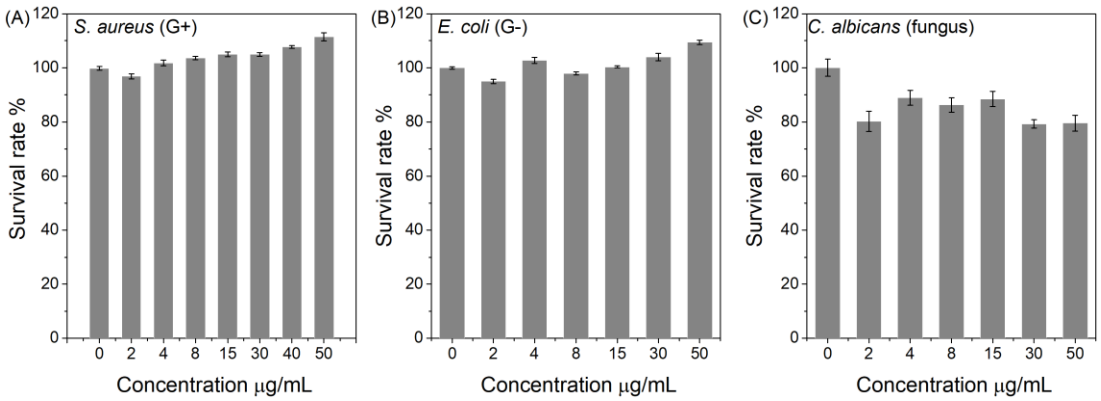

Figure S23. Dark toxicity evaluation of PT10 toward *E. coli* (G-), *S. aureus* (G+) and *C. albicans* (fungus). Error bars = Standard Deviation (n = 3).

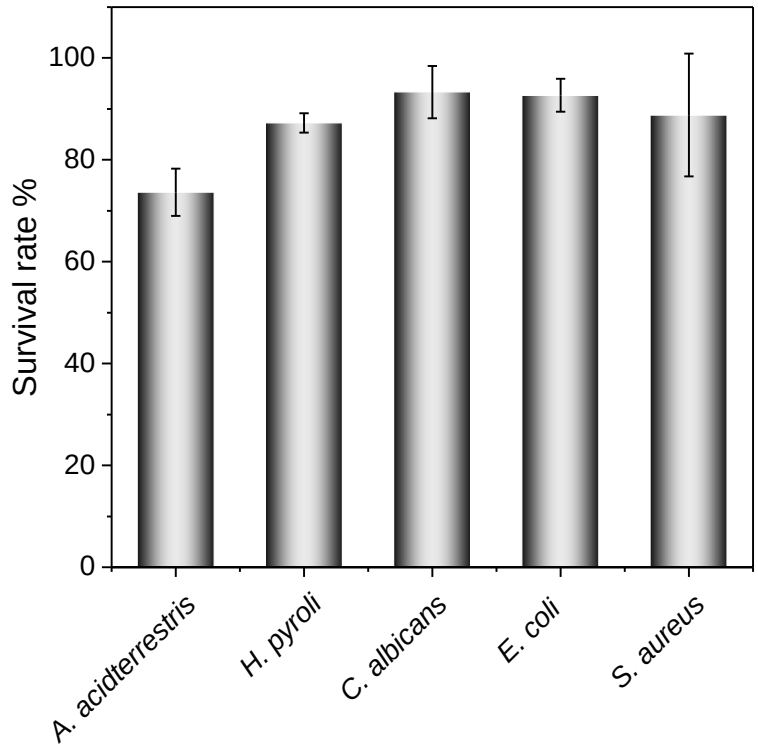

Figure S24. Evaluation the influence of blue light towards various microbials. Error bars = Standard Deviation (n = 3).

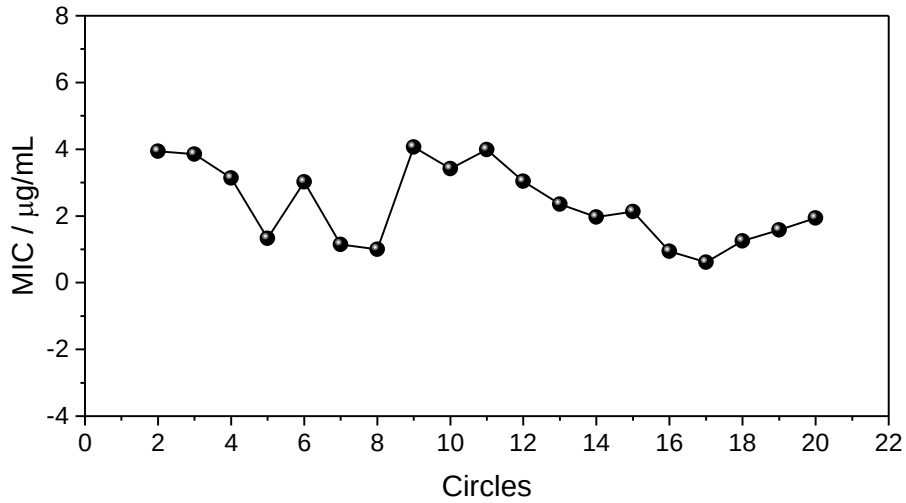

Figure S25. Evaluation of the drug resistance of *C. albicans* against PT10 with blue light illumination. *C. albicans* were passaged in the presence of a sub-lethal dose of PT10 with blue light for indicated generations. The data was obtained from three independent experiments.

5.2 PT10 versus antibiotics

5.2.1 *C. albicans*

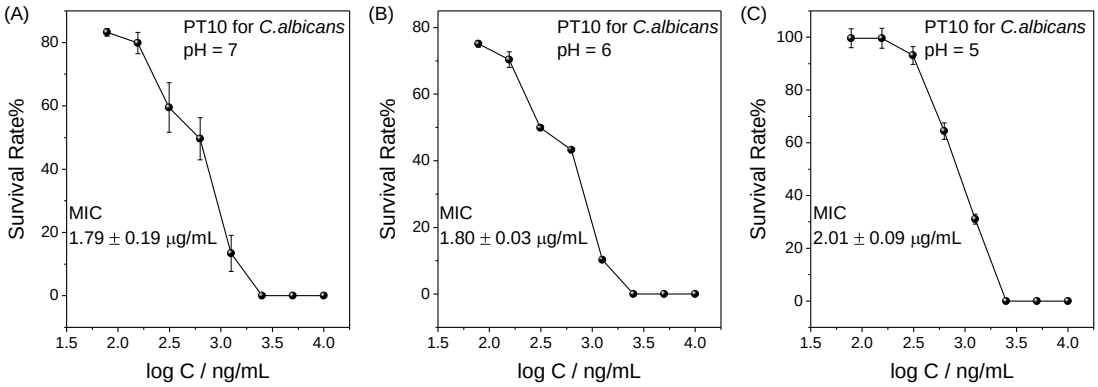

Figure S26. Effects of media pH on the growth inhibition of *C. albicans* by different concentrations of PT10: (A) pH = 7 (MIC = 1.79 ± 0.19 μg/mL); (B) pH = 6 (MIC = 1.80 ± 0.03 μg/mL); and (C) pH = 5 (MIC = 2.01 ± 0.09 μg/mL). Error bars = Standard Deviation (n = 3).

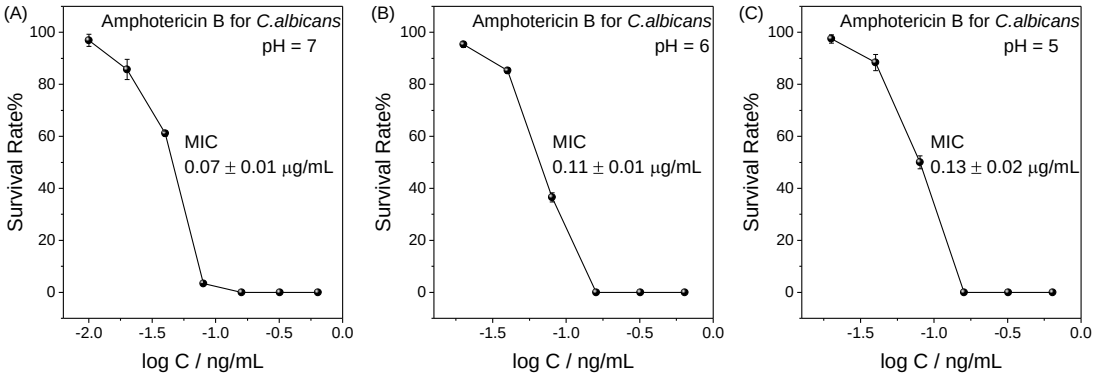

Figure S27. Effects of media pH on the growth inhibition of *C. albicans* by different concentrations of Amphotericin B: (A) pH = 7 (MIC = 0.07 ± 0.01 μg/mL); (B) pH = 6 (MIC = 0.11 ± 0.01 μg/mL); and (C) pH = 5 (MIC = 0.13 ± 0.02 μg/mL). Error bars = Standard Deviation (n = 3).

5.2.2 *penicillin-resistant E. coli*

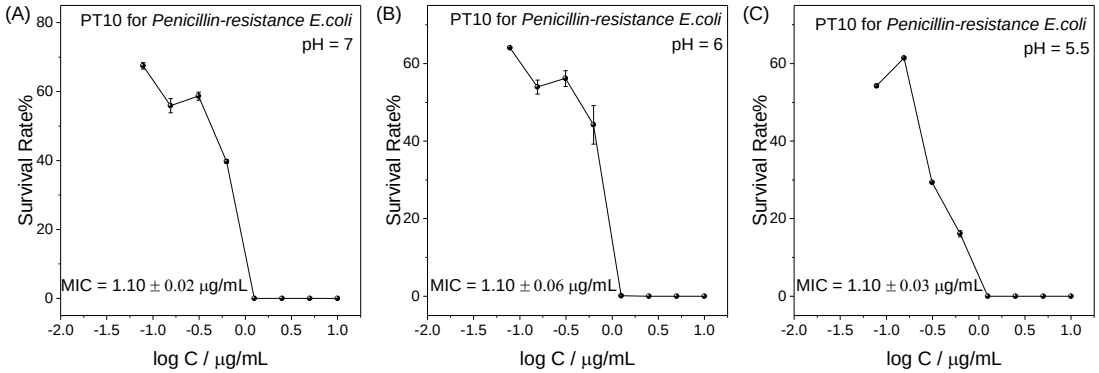

Figure S28. Effects of media pH on the growth inhibition of *penicillin-resistant E. coli* by different concentrations of PT10: (A) pH = 7 (MIC = 1.10 ± 0.02 μg/mL); (B) pH = 6 (MIC = 1.10 ± 0.06 μg/mL); and (C) pH = 5 (MIC = 1.10 ± 0.03 μg/mL) Error bars = Standard Deviation (n = 3).

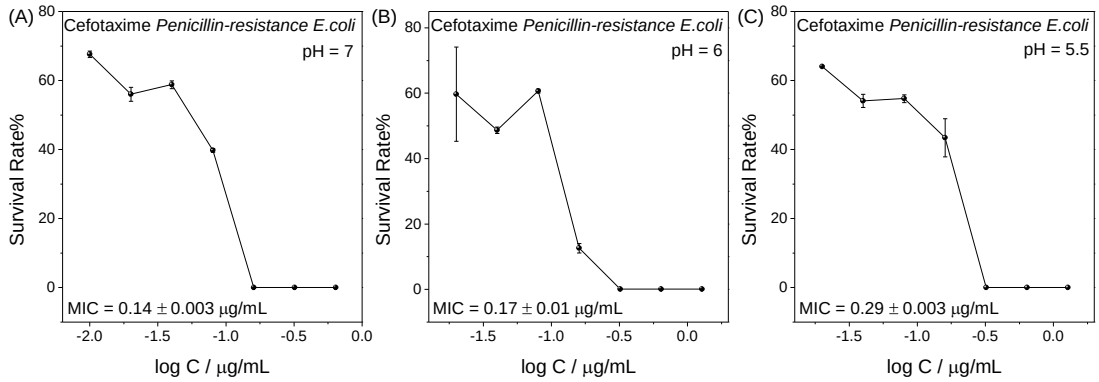

Figure S29. Effects of media pH on the growth inhibition of *penicillin-resistant E. coli* by different concentrations of Cefotaxime: (A) pH = 7 (MIC = 0.14 ± 0.03 μg/mL); (B) pH = 6 (MIC = 0.17 ± 0.01 μg/mL); and (C) pH = 5 (MIC = 0.29 ± 0.003 μg/mL) Error bars = Standard Deviation (n = 3).

5.3 PT10 versus other photosensitizers

5.3.1 *C. albicans*

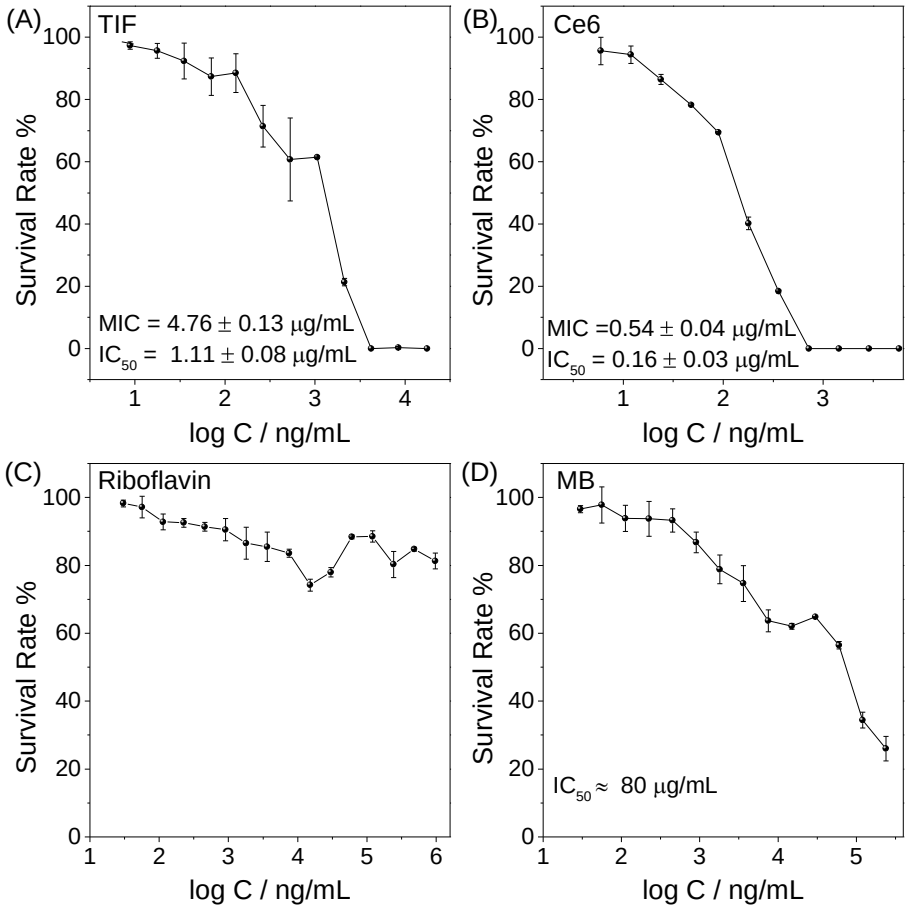

Figure S30. Growth inhibition of *C. albicans* by different concentrations of (A) TIF, (B) Ce6, (C) riboflavin, and (D) MB at pH = 2. Irradiation: 450 nm (LED, 30 mW/cm^2) for 10 min. Error bars = Standard Deviation (n = 3).

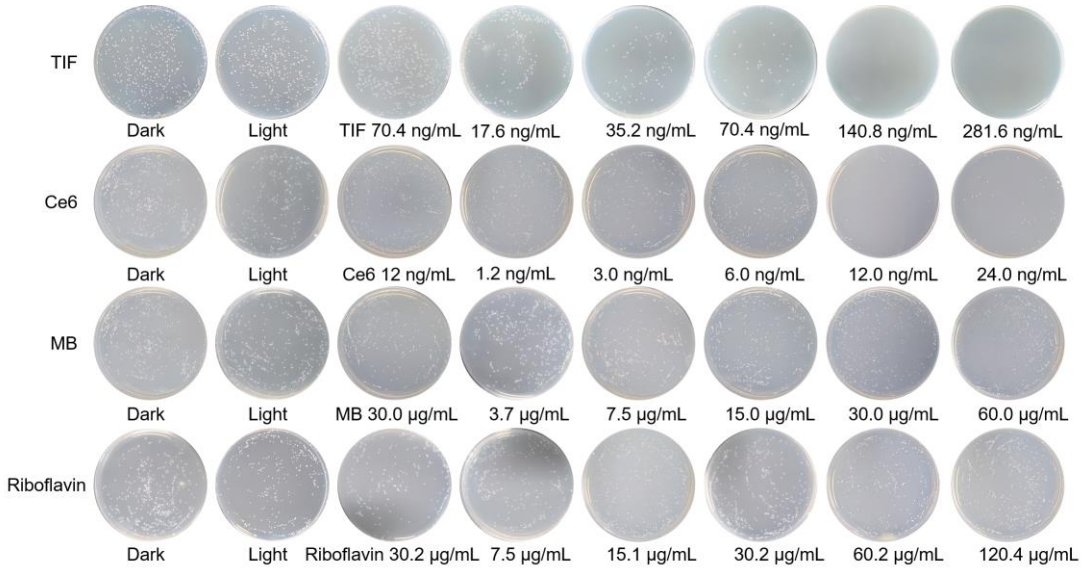

Figure S31. Photographs of *C. albicans* upon treatment with different photosensitizers.

5.3.2 *A. acidterrestris*

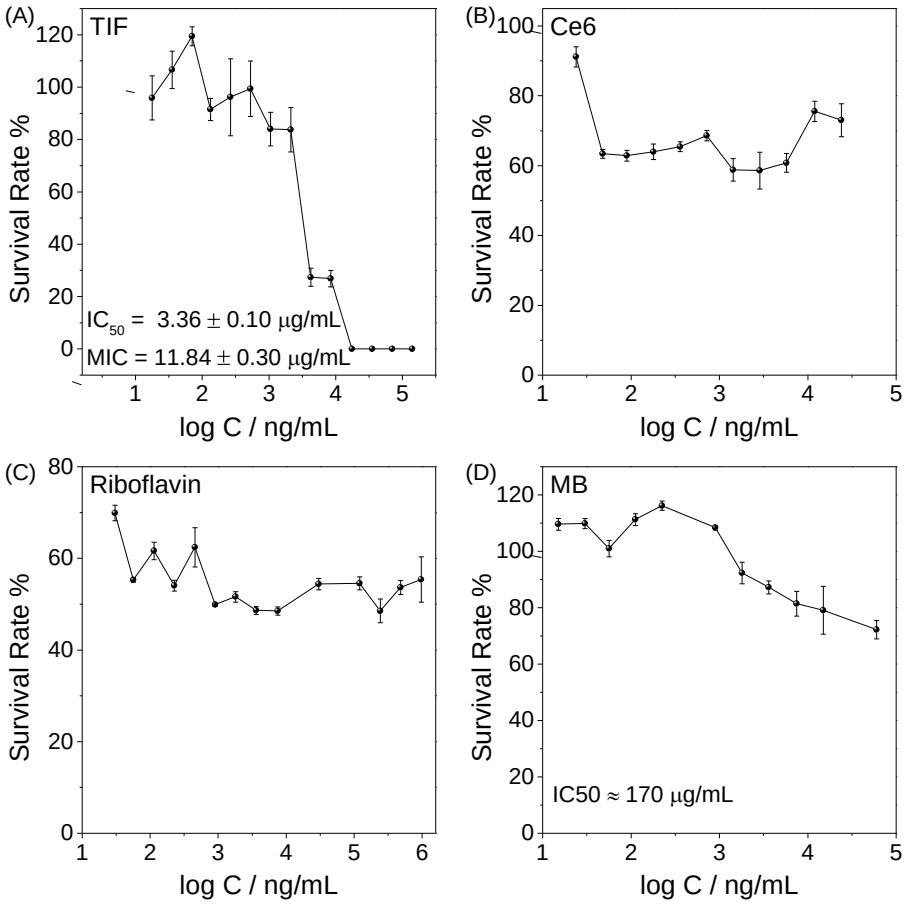

Figure S32. Growth inhibition of *A. acidterrestris* by different concentrations of (A) TIF, (B) Ce6, (C) riboflavin, and (D) MB at pH = 2. Irradiation: 450 nm (LED, 30 mW/cm^2) for 10 min. Error bars = Standard Deviation (n = 3).

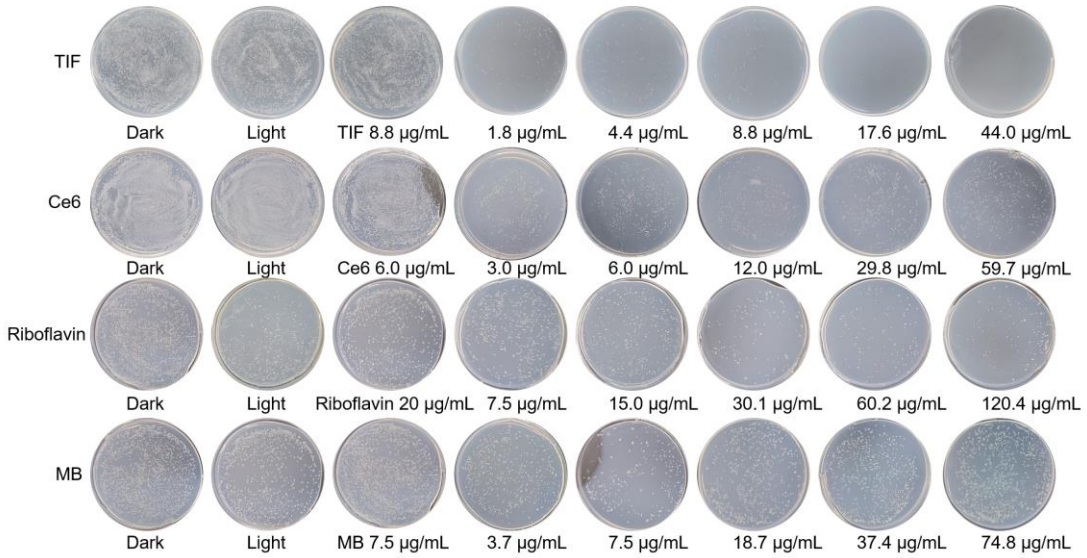

Figure S33. Photographs of *A. acidterrestris* upon treatment with different photosensitizers.

5.3.3 *H. pylori*

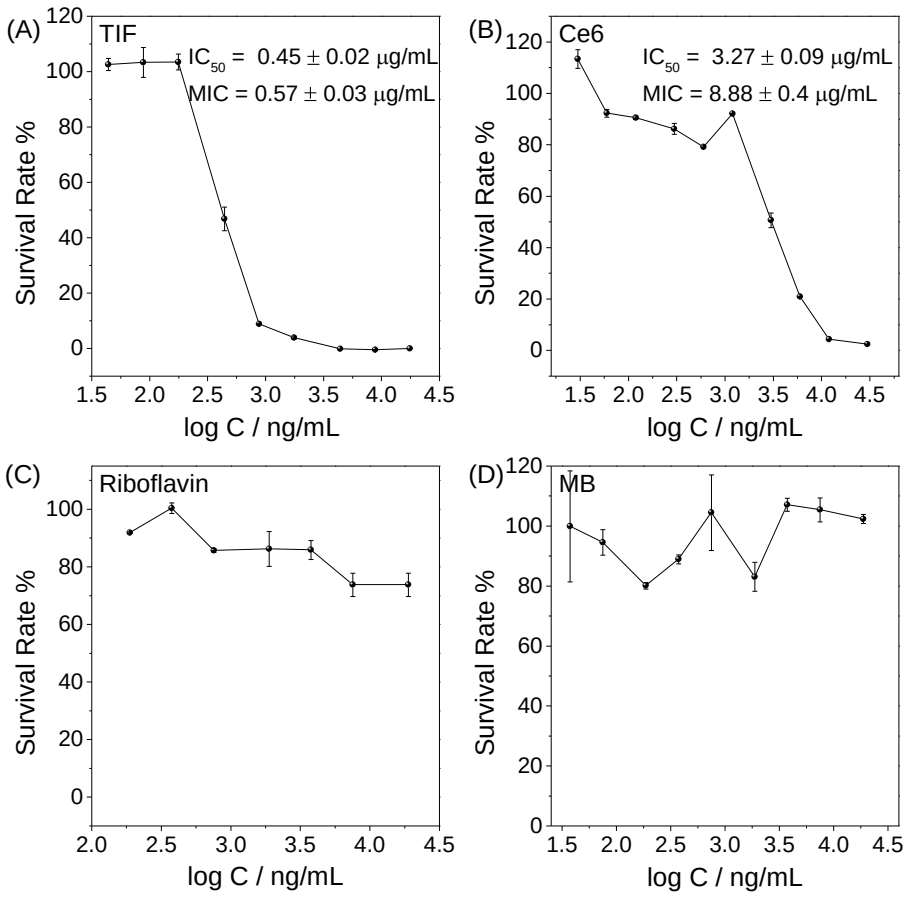

Figure S34. Growth inhibition of *H. pylori* by different concentrations of (A) TIF, (B) Ce6, (C) riboflavin, and (D) MB at pH = 2. Irradiation: 450 nm (LED, 30 mW/cm^2) for 10 min. Error bars = Standard Deviation (n = 3).

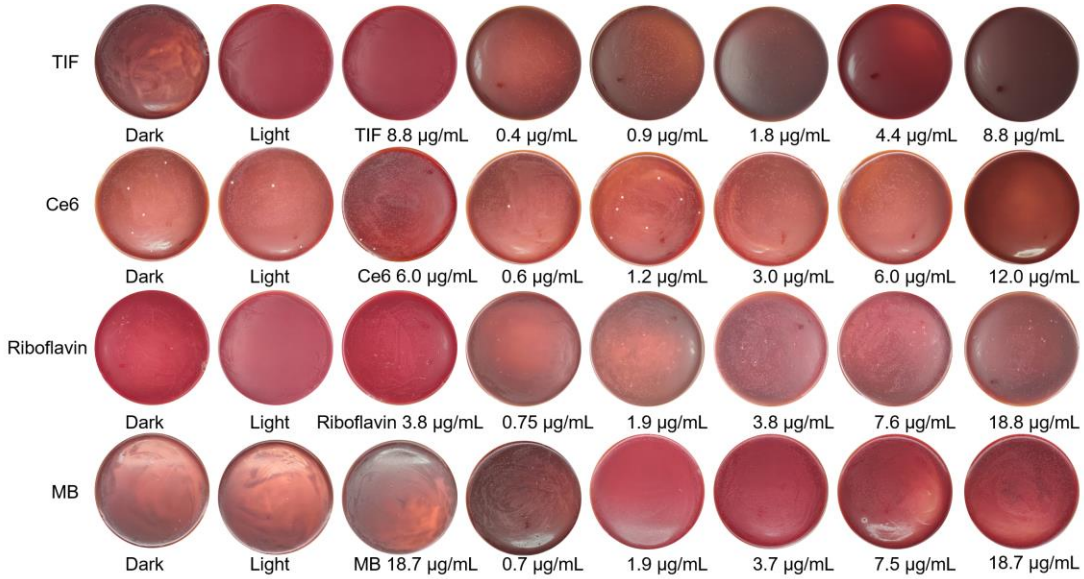

Figure S35. Photographs of *H. pylori* upon treatment with different photosensitizers.

Table S8. Comparison of antimicrobial performance of PT10 with other photo-antimicrobials

Microbials name	Photo-antimicrobial	MIC_{100} μg/mL	MIC/ Abs_{max}	IC_{50} μg/mL	IC_{50}/Abs_{max}
C. albicans (Fungus)	PT10	4.21 ±0.25	0.051	1.09 ±0.01	0.013
	TIF	4.76 ±0.13	0.325	1.11 ±0.08	0.075
	Ce6	0.54 ±0.04	0.140	0.16 ±0.04	0.040
	Riboflavin	-	-	-	-
	MB	-	-	~220	>5
A. acidoterrestris (G+)	PT10	1.4 ±0.14	0.017	1.20 ±0.01	0.014
	TIF	11.84 ±0.30	0.796	3.36 ±0.10	0.226
	Ce6	-	-	-	-
	Riboflavin	-	-	-	-
	MB	-	-	~460	>5
H. pylori (G-)	PT10	2.64 ±0.39	0.032	0.65 ±0.24	0.008
	TIF	0.45 ±0.02	0.037	0.45 ±0.02	0.029
	Ce6	8.88 ±0.4	>5	3.27 ±0.09	0.844
	Riboflavin	-	-	-	-
	MB	-	-	-	-

5.3.4 *M. aeruginosa*

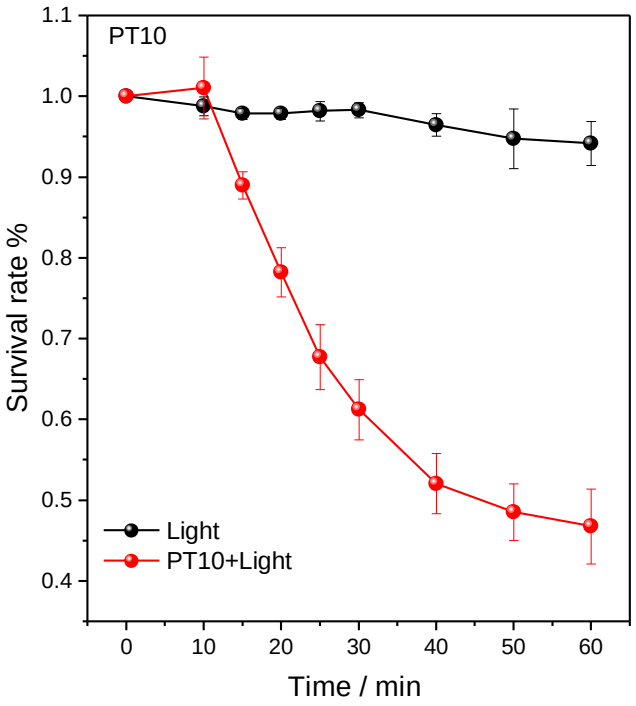

Figure S36. Time courses of growth inhibition of *M. aeruginosa* by PT10 (abs = 0.3) in the absence and presence of light. Irradiation: 450 nm LED, 30 mW/cm^2. Error bars = Standard Deviation (n = 3).

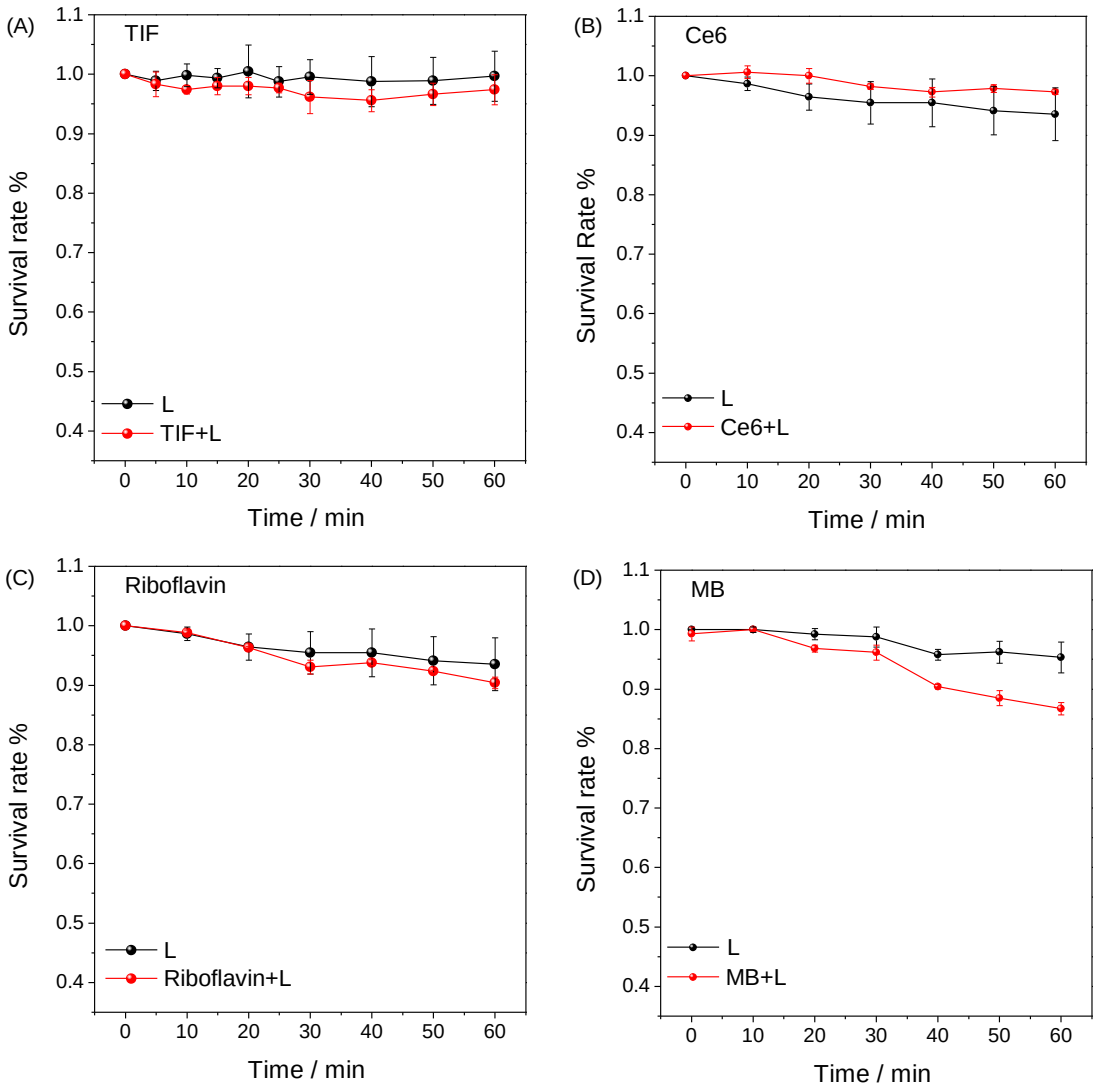

Figure S37. Time courses of the growth inhibition of *M. aeruginosa* by different photosensitizers with the same absorbance at maximum peak (abs = 0.3): (A) TIF, (B) Ce6, (C) riboflavin, and (d) MB at pH = 12; Irradiation: 450 nm LED, 30 mW/cm^2. Error bars = Standard Deviation (n = 3).

5.4 Interaction between PT10 and *C. albicans*

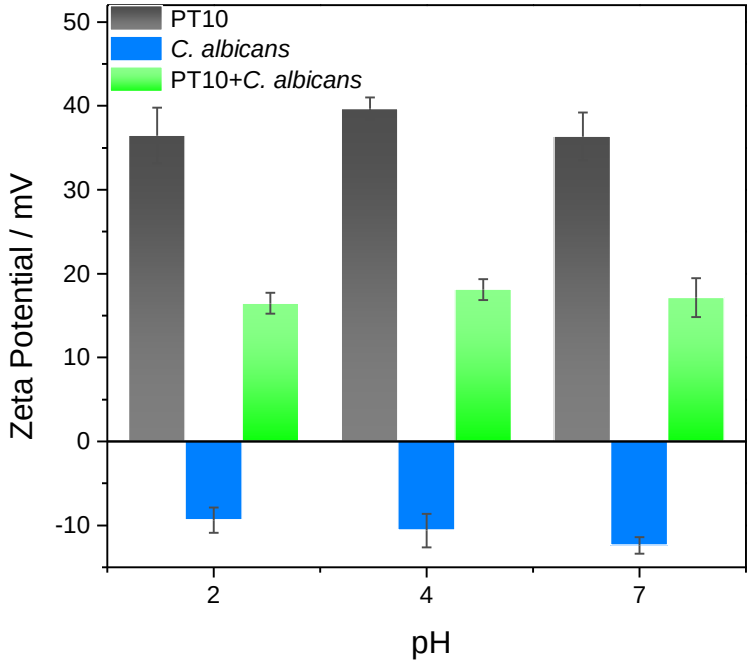

Figure S38. Zeta potentials of PT10, *C. albicans*, and *C. albicans* + PT10 at different pH: (A) pH = 2; (B) pH = 4; and (C) pH = 7.

Section S6. *In vivo* PDI performance of PT10

6.1 Biocompatibility of PT10

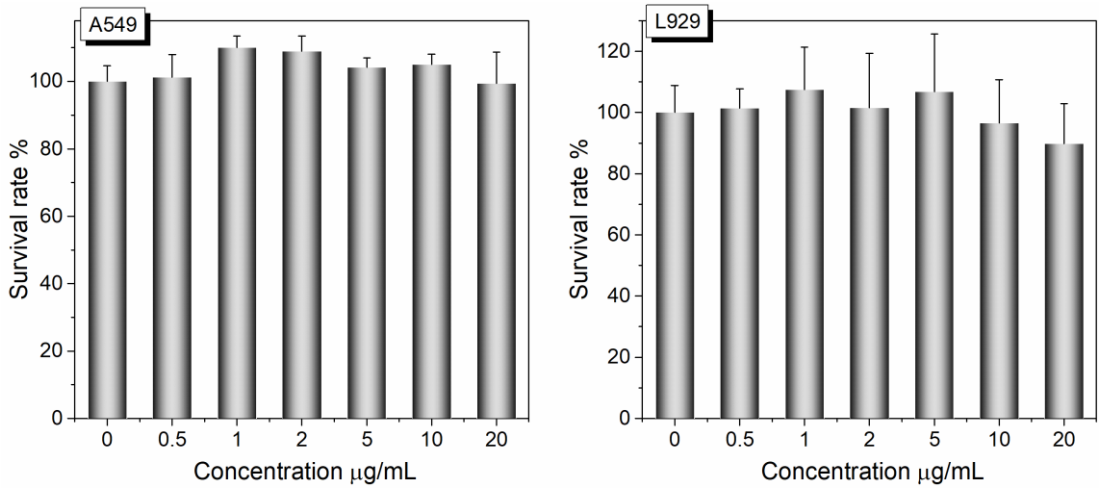

Figure S39. The biocompatibility of PT10 towards to (A) A549 cells, and (B) L929 cells assessed by CCK-8 assay. Error bars = Standard Deviation (n = 6).

6.2 Pathology index and Body weight of the mice

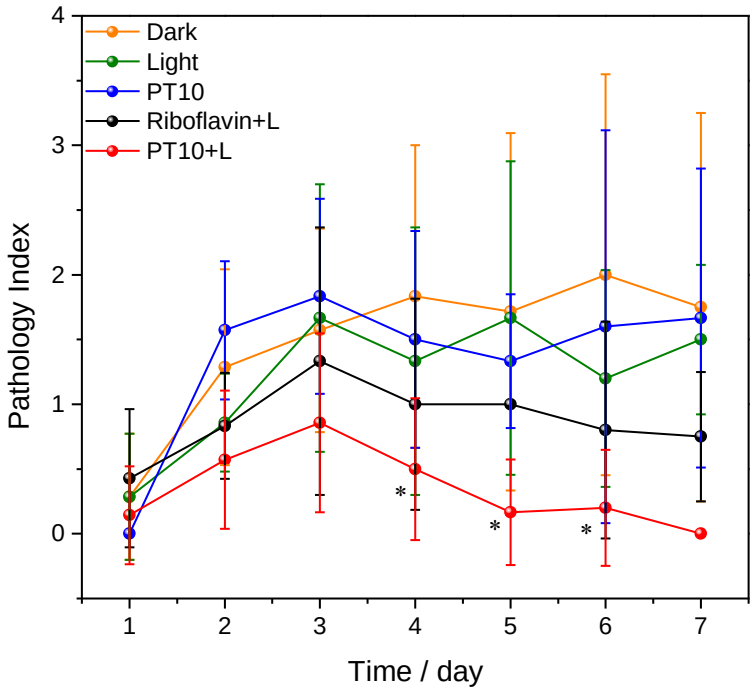

Figure S40. Pathology index analysis of the mice of different groups at different time intervals (* $p < 0.05$). Error bars represent standard deviation, n =6 independent replicates.

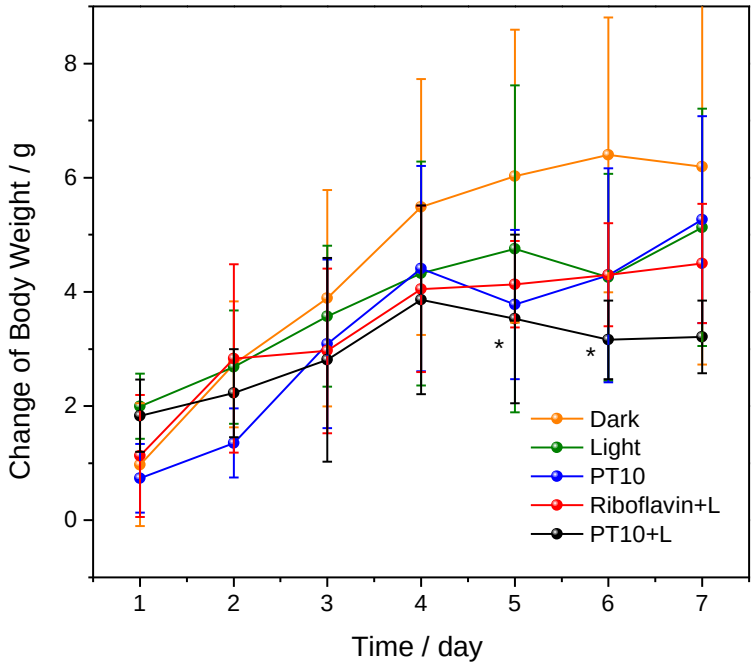

Figure S41. Body weight of mice with/without treatment at different time intervals (* $p < 0.05$). Error bars represent standard deviation, n =6 independent replicates.

References

1 D. Schmaljohann, *Adv. Drug Delivery Rev.*, 2006, **58**, 1655.

2 C. S. Danby, D. Boikov, R. Rautemaa-Richardson and J. D. Sobel, *Antimicrob Agents Ch*, 2012, **56**, 1403.

3 V. Thongboonkerd, S. Mungdee and W. Chiangjong, *J. Proteome. Res.*, 2009, **8**, 3206.

4 Y. J. Luo, C. Li, W. C. Zhu, X. J. Zheng, Y. Huang and Z. Y. Lu, *Angew. Chem., Int. Ed.*, 2019, **58**, 6280.

5 S. C. Doney, V. J. Fabry, R. A. Feely and J. A. Kleypas, *Annu. Rev. Mar. Sci.*, 2009, **1**, 169.

6 T. J. Shao, J. B. Zhao, Q. Zhou, Z. B. Dong and Y. D. Ma, *J. Geogr. Sci.*, 2012, **22**, 479.

7 K. H. Johannesson, W. B. Lyons, K. J. Stetzenbach and R. H. Byrne, *Aquat. Geochem.*, 1995, **1**, 157.

8 B. W. Fouke, *Sedimentology*, 2011, **58**, 170.

9 J. Retka, G. Rzepa, T. Bajda and L. Drewniak, *Minerals*, 2020, **10**, 1061.

10 J. H. Guo, X. J. Liu, Y. Zhang, J. L. Shen, W. X. Han, W. F. Zhang, P. Christie, K. W. T. Goulding, P. M. Vitousek and F. S. Zhang, *Science*, 2010, **327**, 1008.

11 Y. H. Lang, S. H. Wu, Q. Yang, Y. J. Luo, X. Jiang and P. Wu, *Anal. Chem.*, 2021, **93**, 9737.

12 F. Cheng, N. Tang, J. Chen and L. Chen, *Sens. Actuators, B*, 2012, **171**, 102.

13 N. V. Solis and S. G. Filler, *Nat. Protoc.*, 2012, **7**, 637.

14 W. C. Sun, K. R. Gee, D. H. Klaubert and R. P. Haugland, *Journal of Organic Chemistry*, 1997, **62**, 6469.

15 W. Zhang, M. Caldarola, B. Pradhan and M. Orrit, *Angew. Chem., Int. Ed.*, 2017, **56**, 3566.

16 (a)B. Cunderlikova, L. Gangeskar and J. Moan, *Journal of Photochemistry and Photobiology, B: Biology*, 1999, **53**, 81; (b)S. Paul, S. Selvam, P. W. S. Heng and L. W. Chan, *J. Fluoresc.*, 2013, **23**, 1065.

17 F. Miiller, *CRC, Boca Raton*, 1991, **https://doi.org/10.1201/9781351070577**.

18 (a)T. Lu and F. Chen, *J. Mol. Graphics Modell.*, 2012, **38**, 314; (b)T. Lu and F. Chen, *J. Comput. Chem.*, 2012, **33**, 580.

19 J. E. Szulejko and T. B. McMahon, *J. Am. Chem. Soc.*, 1993, **115**, 7839.

20 Y. Lang, S. Wu, Q. Yang, Y. Luo, X. Jiang and P. Wu, *Analytical Chemistry*, 2021, **93**, 9737.

21 Y. Zhang and H. Goerner, *Dyes Pigm.*, 2009, **83**, 174.

22 M. Gonzalez-Bejar, P. Montes-Navajas, H. Garcia and J. C. Scaiano, *Langmuir*, 2009, **25**, 10490.

23 M. Westberg, M. Bregnhoj, M. Etzerodt and P. R. Ogilby, *J. Phys. Chem. B*, 2017, **121**, 2561.